

Introduction; diffraction theory, kinematic and dynamical, new trends,.. ..

Diffraction Workshop Trondheim

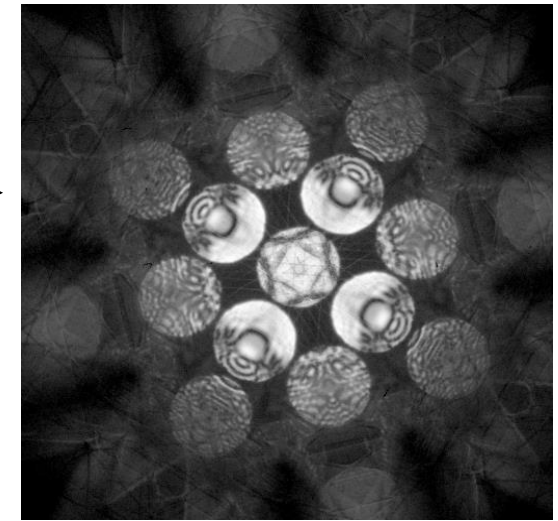
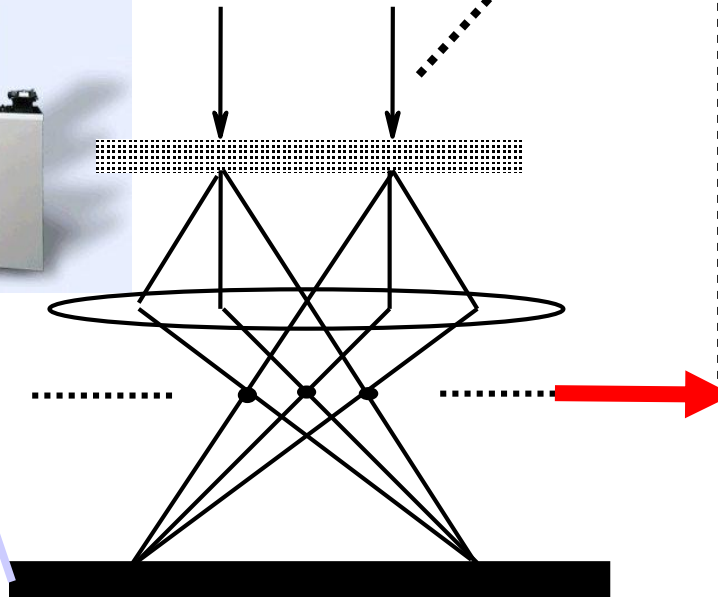
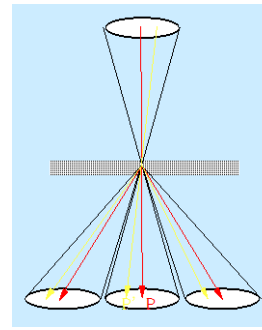
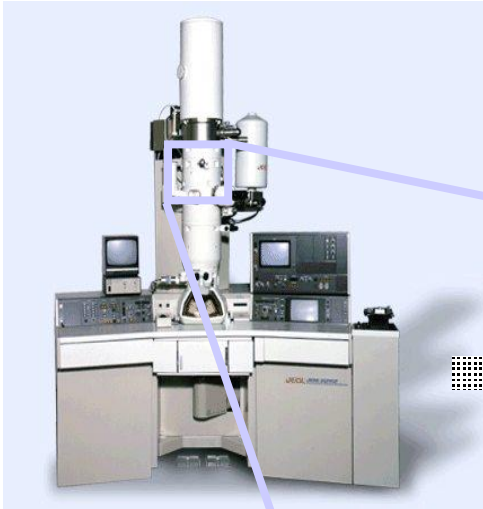
‘The reciprocal reality: electron diffraction in the new age’

Randi Holmestad

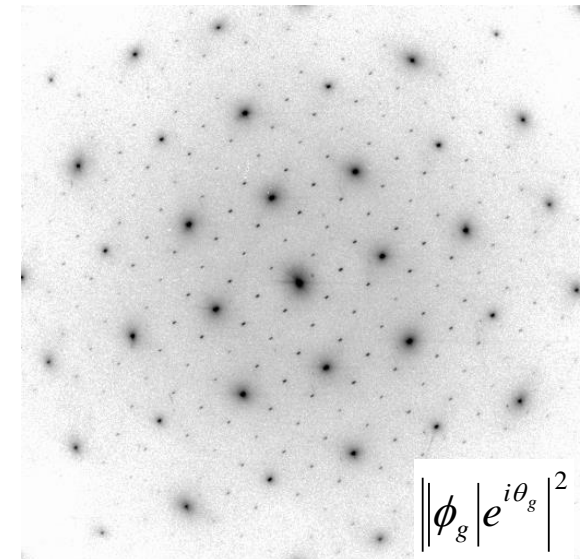
Outline

- **Introduction to electron diffraction**
 - Basics in diffraction
 - Electron versus X-ray diffraction
 - SAED → CBED; geometry of CBED
- **Kinematic & dynamic (many beam) simulations**
 - Kinematic diffraction
 - Precession method: Pseudo-kinematic diffraction
 - Dynamical theory; two beam case
- **Experimental considerations**
 - Inelastic scattering, energy filtering
- **Refinement from CBED intensities**
 - Structure factors U_g and their relation to charge density
 - Refining low order U_g using dynamic diffraction intensities
- **Solving structures?**
- **'New' trends**
 - SPED, Scanning CBED, Coherent diffraction - Ptychography

Electron crystallography



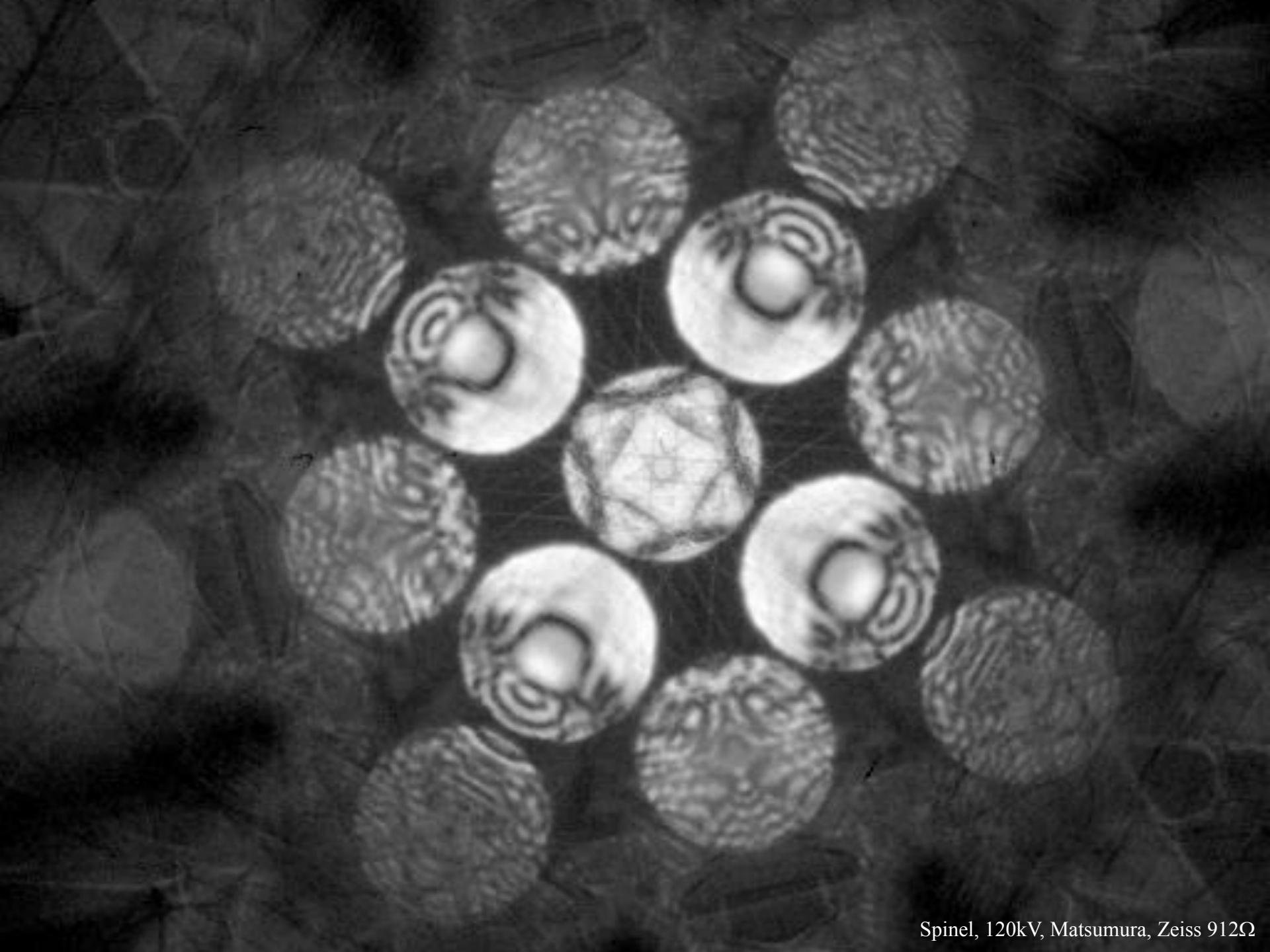
Spinel, Matsumura



$$\left| \phi_g e^{i\theta_g} \right|^2$$

(magnetite, LN)

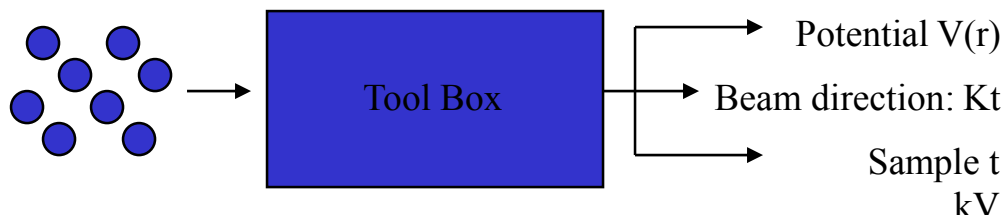
Electron crystallography is the use of different information by electron scattering to study the ordered solid state (crystalline state).



Spinel, 120kV, Matsumura, Zeiss 912Ω

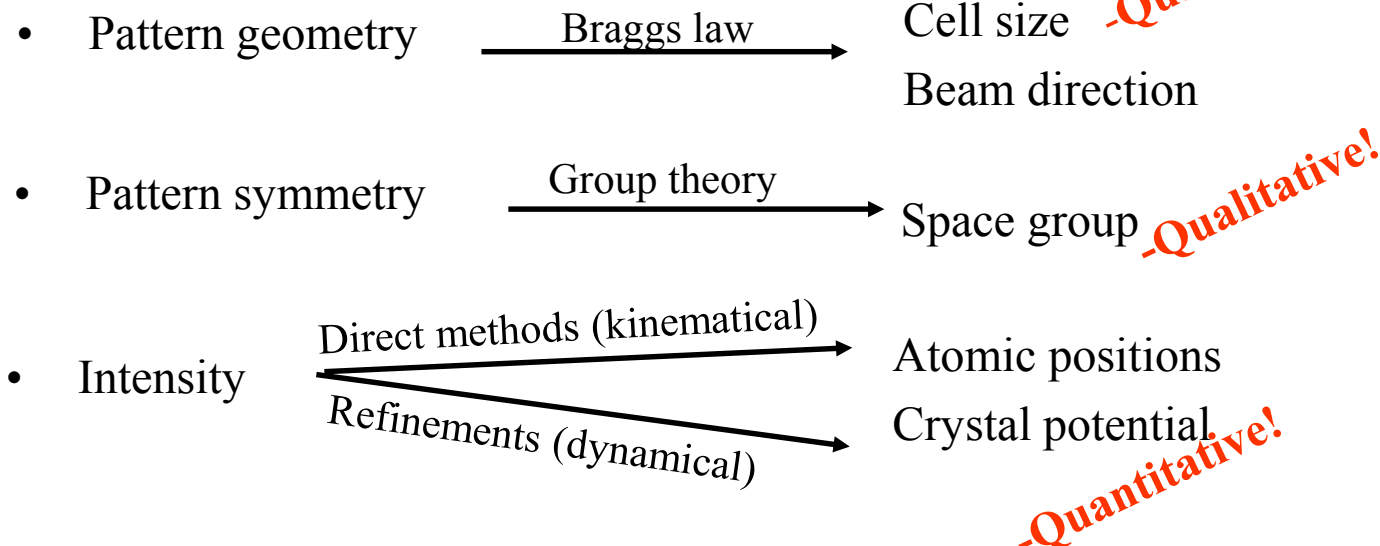
Structure information from electron diffraction

Experiment :

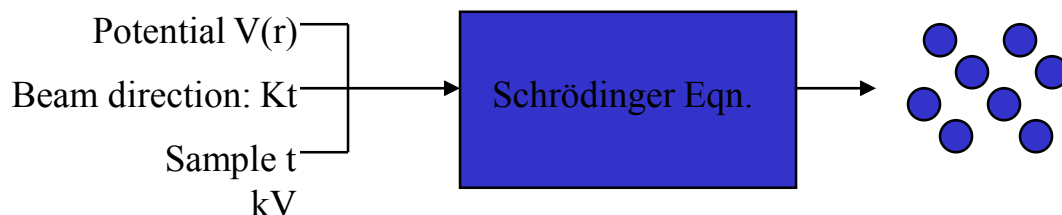


Problem of inversion

Tool box:



Simulation :



Diffraction in TEM

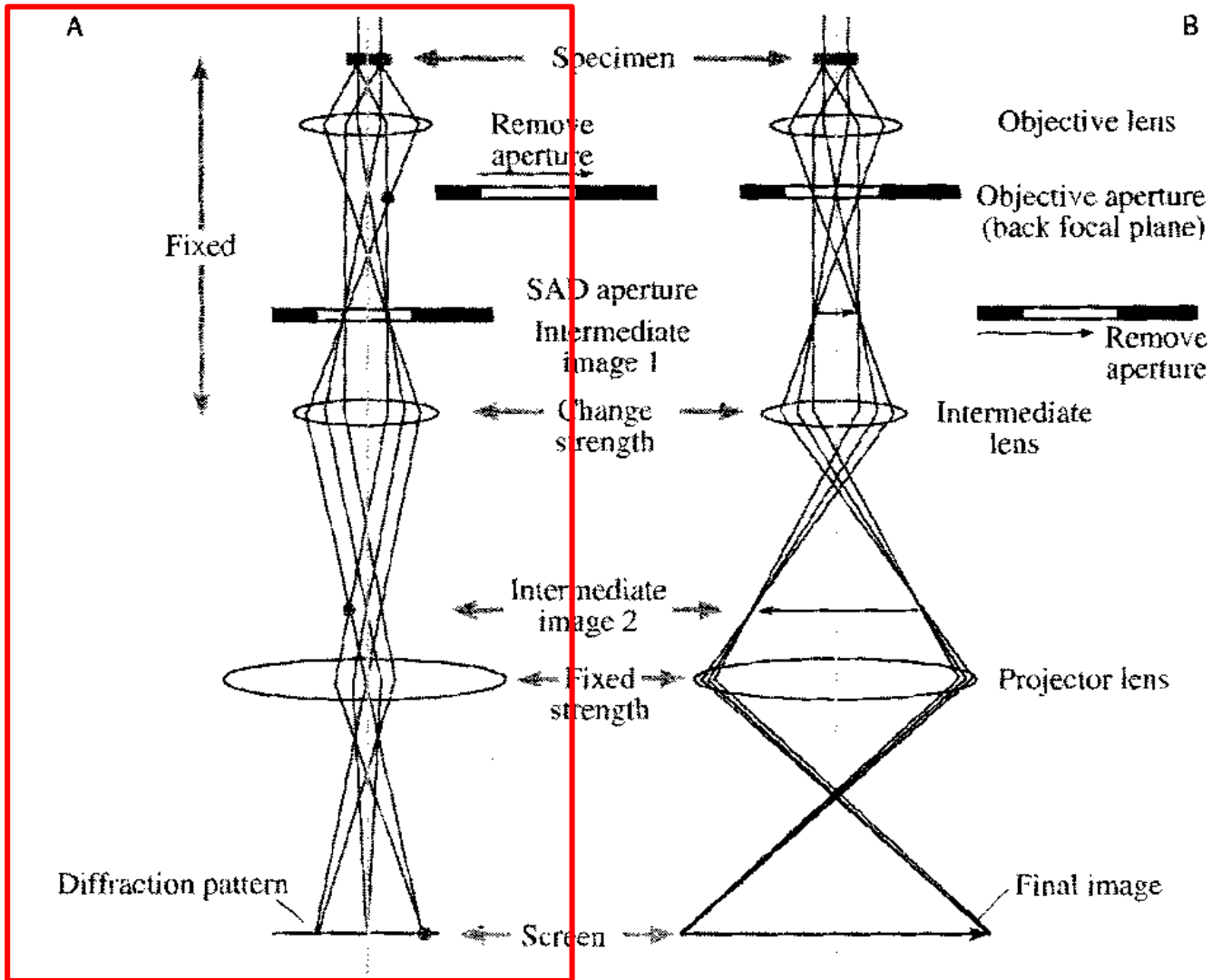
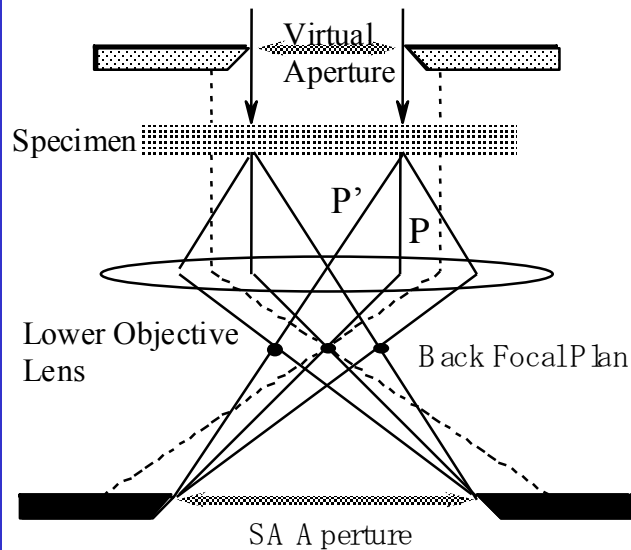
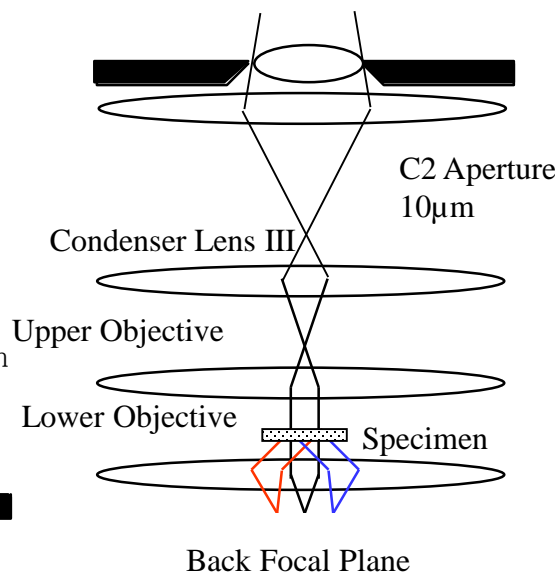


Figure 9.12. The two basic operations of the TEM imaging system involve (A) projecting the diffraction pattern on the viewing screen and (B) projecting the image onto the screen. In each case the intermediate lens selects either the back focal plane or the image plane of the objective lens as its object.

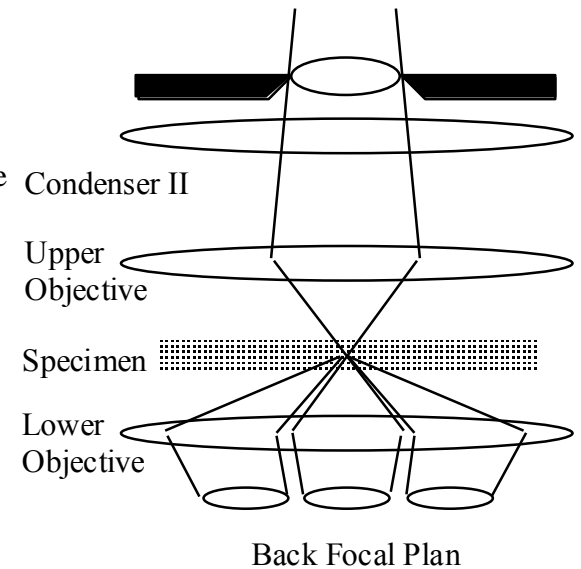
Choice of electron illumination and diffraction techniques



a) **Selected Area Electron Diffraction**



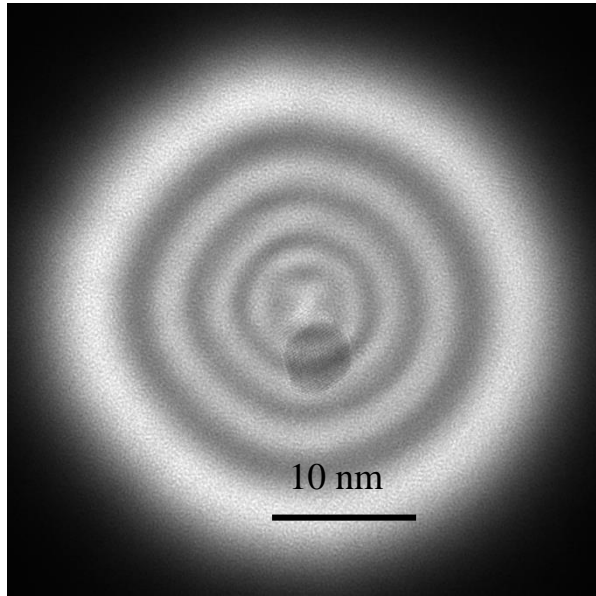
b) **Electron nanobeam diffraction**



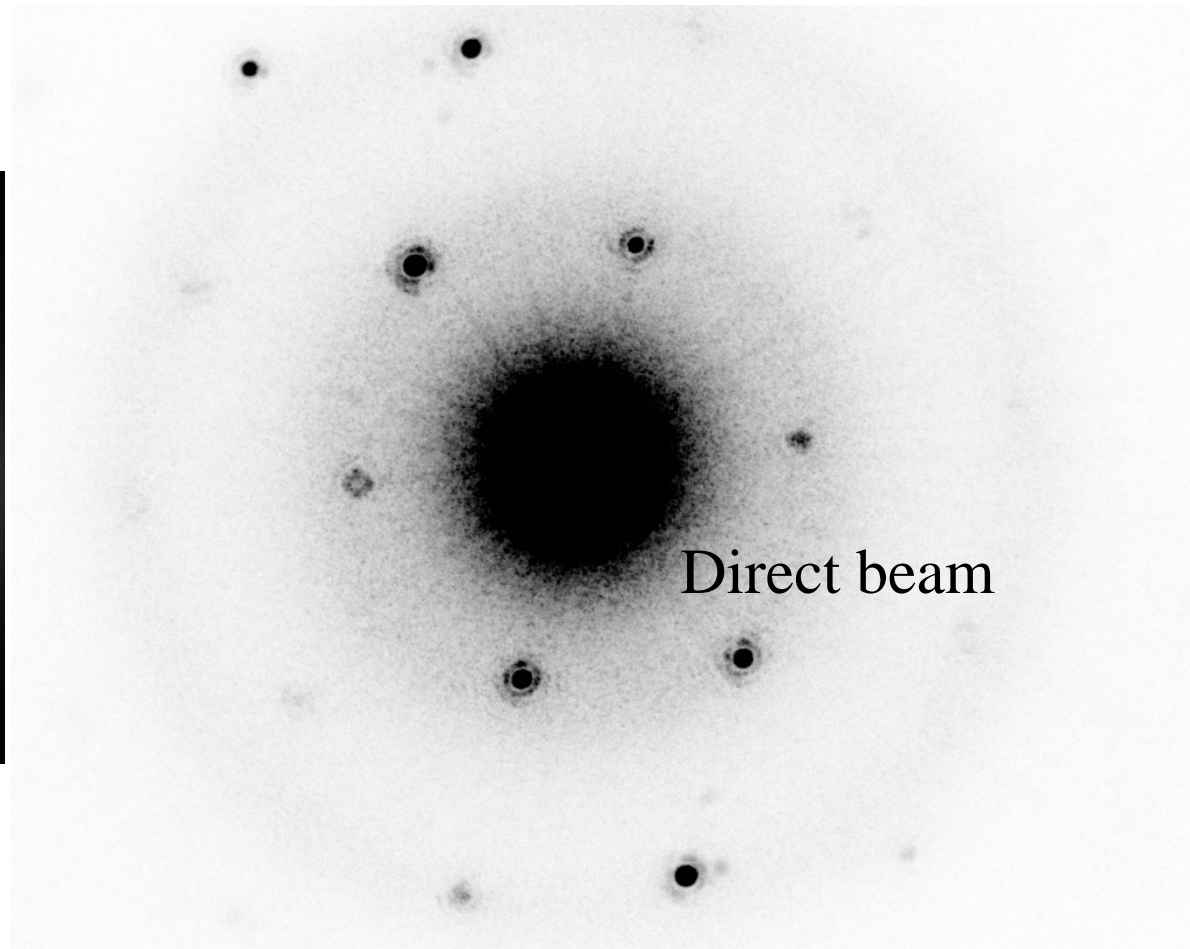
c) **Convergent Beam Electron Diffraction (CBED)**

Other electron diffraction techniques: Large angle CBED, Precession electron diffraction

Example of nanobeam illumination



Au nanocrystal

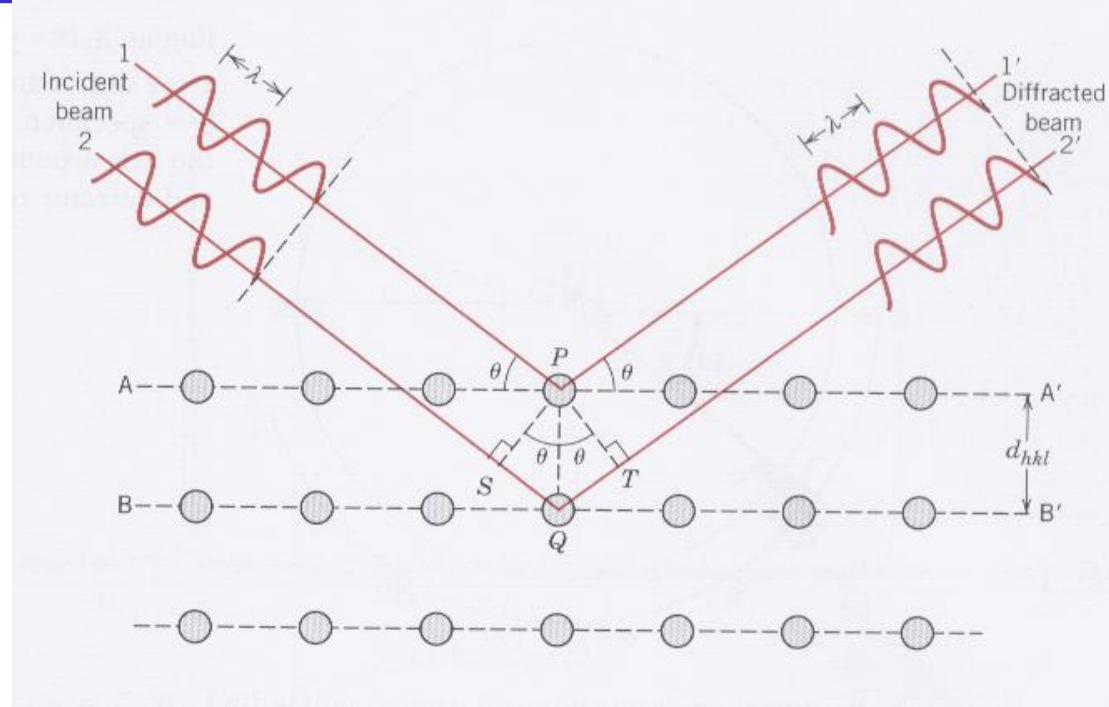


Direct beam

Braggs equation

● atoms in a crystal,
separated with a distance d_{hkl}

The two scattered beams 1 and 2 are in phase only if the path difference between them is equal a whole number of wave lengths.

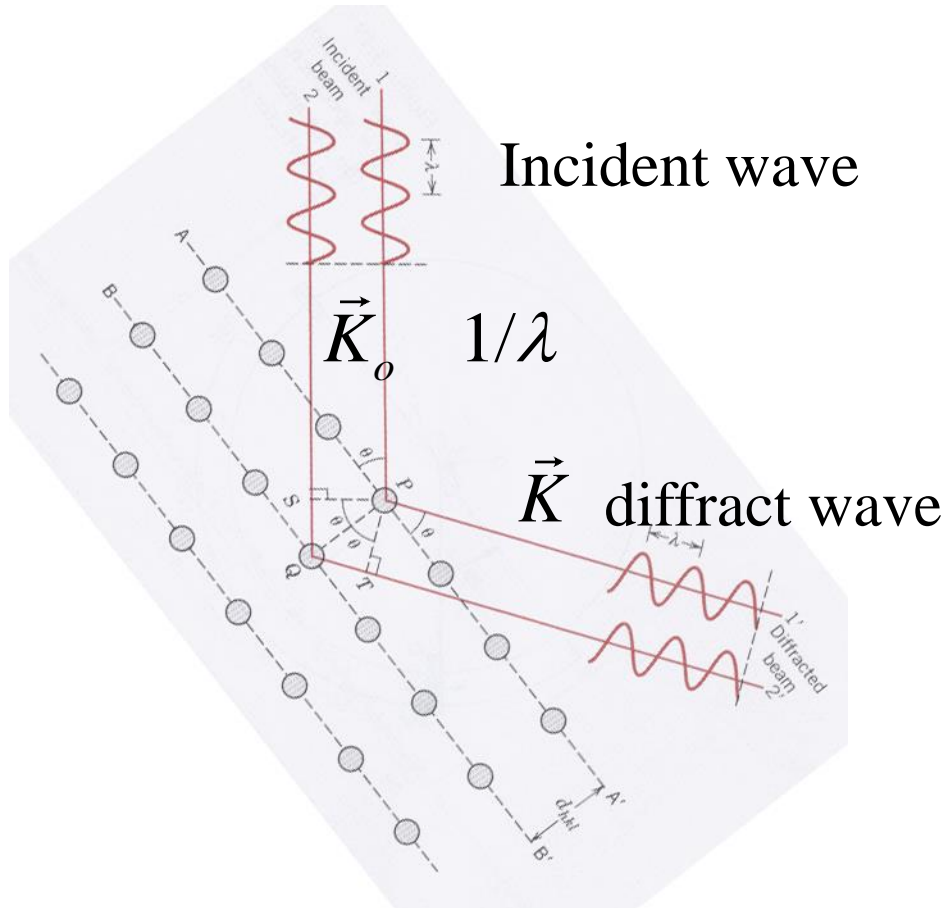


$$n\lambda = d_{hkl} \sin \theta + d_{hkl} \sin \theta = 2d_{hkl} \sin \theta$$

Braggs equation tells how the reflected beams depends on the wavelength λ , the spacing of the planes of atoms d_{hkl} and the angle of incidence of the beam θ .

For transmission electron diffraction, beams are diffracted, not reflected – beams are transmitted with $\theta \sim \text{mrad}$

Inside the TEM



(Actual diffraction angle is much smaller)

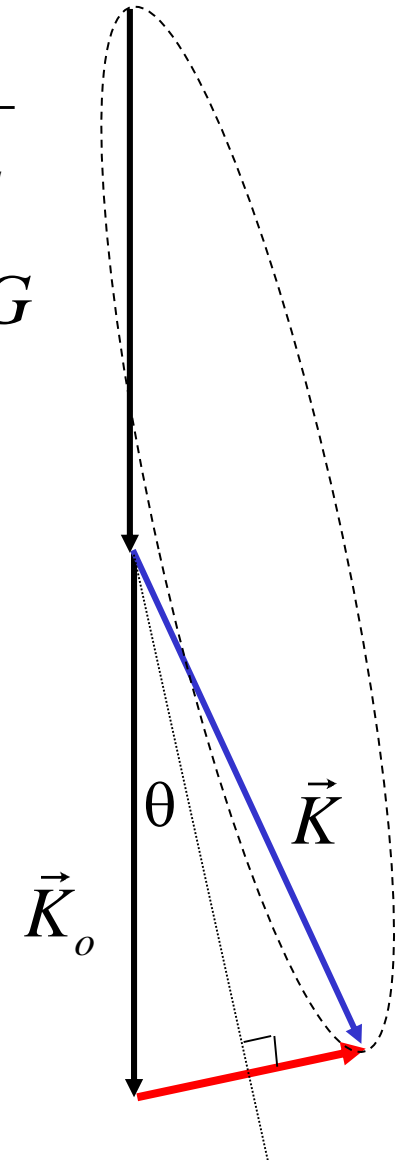
Rewrite Bragg's law in 3D
(Laue equation)

$$2 \frac{1}{\lambda} \sin \theta = \frac{n}{d_{hkl}}$$

$$2 |\vec{K}| \sin \theta = nG$$

$$|\vec{K}_o| = |\vec{K}|$$

$$\vec{K} - \vec{K}_o = \vec{g}$$



Reciprocal space

The reciprocal lattice is a geometrical construction which gives a physical picture of the diffraction geometries. (hkl) designate planes in the real lattice. In a reciprocal lattice, the **reciprocal lattice points (relpoints)** are labeled (or indexed) the same, since they represent the **planes** in the real lattice. The dimension of the reciprocal space is $1/d_{hkl}$, where d_{hkl} is the spacing between (hkl) crystal planes.

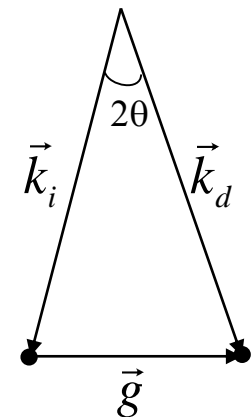
$$\vec{g}_{hkl} = h\vec{a}^* + k\vec{b}^* + l\vec{c}^* \quad \left| \vec{g}_{hkl} \right| = g_{hkl} = 1/d_{hkl}$$

NB! each point in the reciprocal lattice represents a set of planes!

The Laue condition is Braggs equation in reciprocal space

$$\vec{k}_d - \vec{k}_i = \vec{g}$$

$$\left| \vec{k}_i \right| = \left| \vec{k}_d \right| = 1/\lambda$$



Reciprocal Lattice Vectors

Reciprocal space lattice vectors

$$\vec{a}^* = \frac{\vec{b} \times \vec{c}}{V_{Cell}}, \vec{b}^* = \frac{\vec{c} \times \vec{a}}{V_{Cell}}, \vec{c}^* = \frac{\vec{a} \times \vec{b}}{V_{Cell}}$$

$$V_{Cell} = (\vec{a} \times \vec{b}) \cdot \vec{c}$$

$$\vec{g} = h\vec{a}^* + k\vec{b}^* + l\vec{c}^* \quad |\vec{g}| = 1/d_{hkl}$$

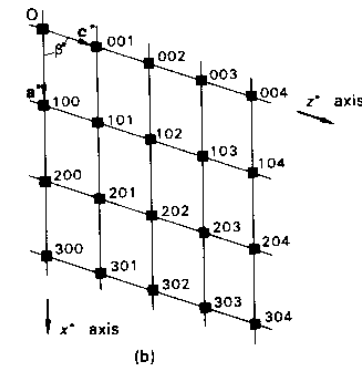
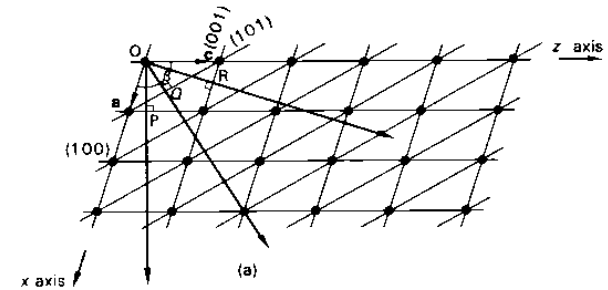
h, k, l , Miller indices, plane normal direction

Relationship between real and reciprocal space

$$\vec{a}^* \cdot \vec{a} = 1, \vec{a}^* \cdot \vec{b} = 0, \vec{a}^* \cdot \vec{c} = 0$$

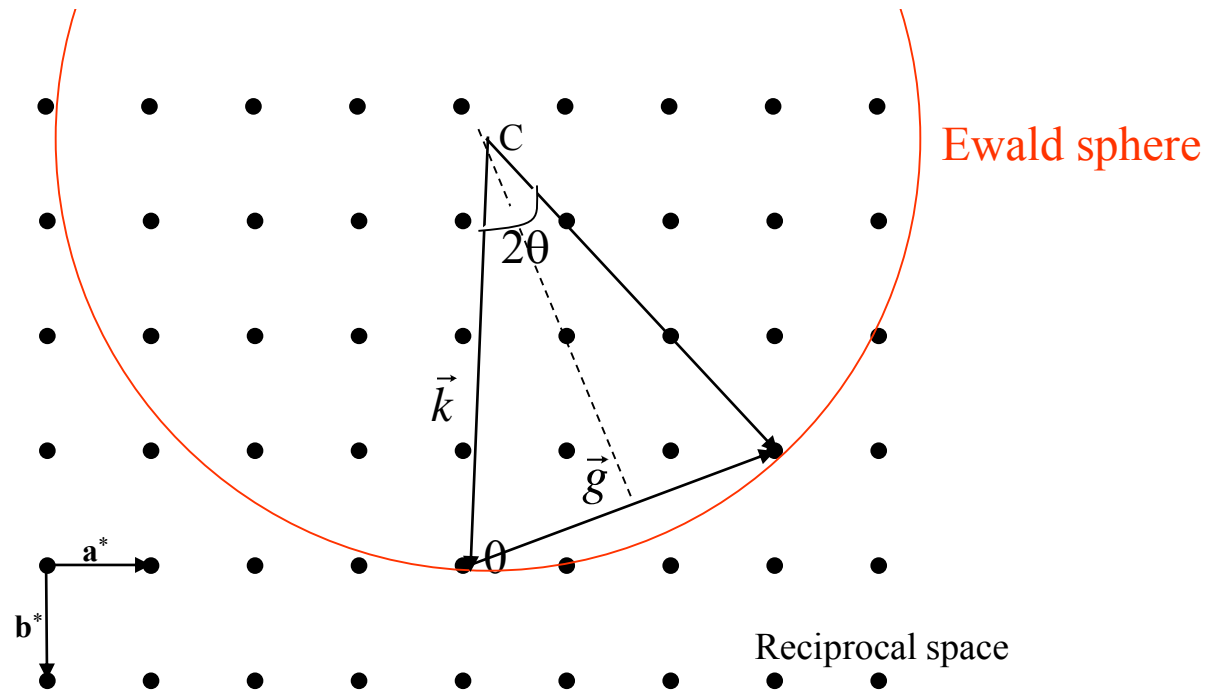
$$\vec{b}^* \cdot \vec{a} = 0, \vec{b}^* \cdot \vec{b} = 1, \vec{b}^* \cdot \vec{c} = 0$$

$$\vec{c}^* \cdot \vec{a} = 0, \vec{c}^* \cdot \vec{b} = 0, \vec{c}^* \cdot \vec{c} = 1$$



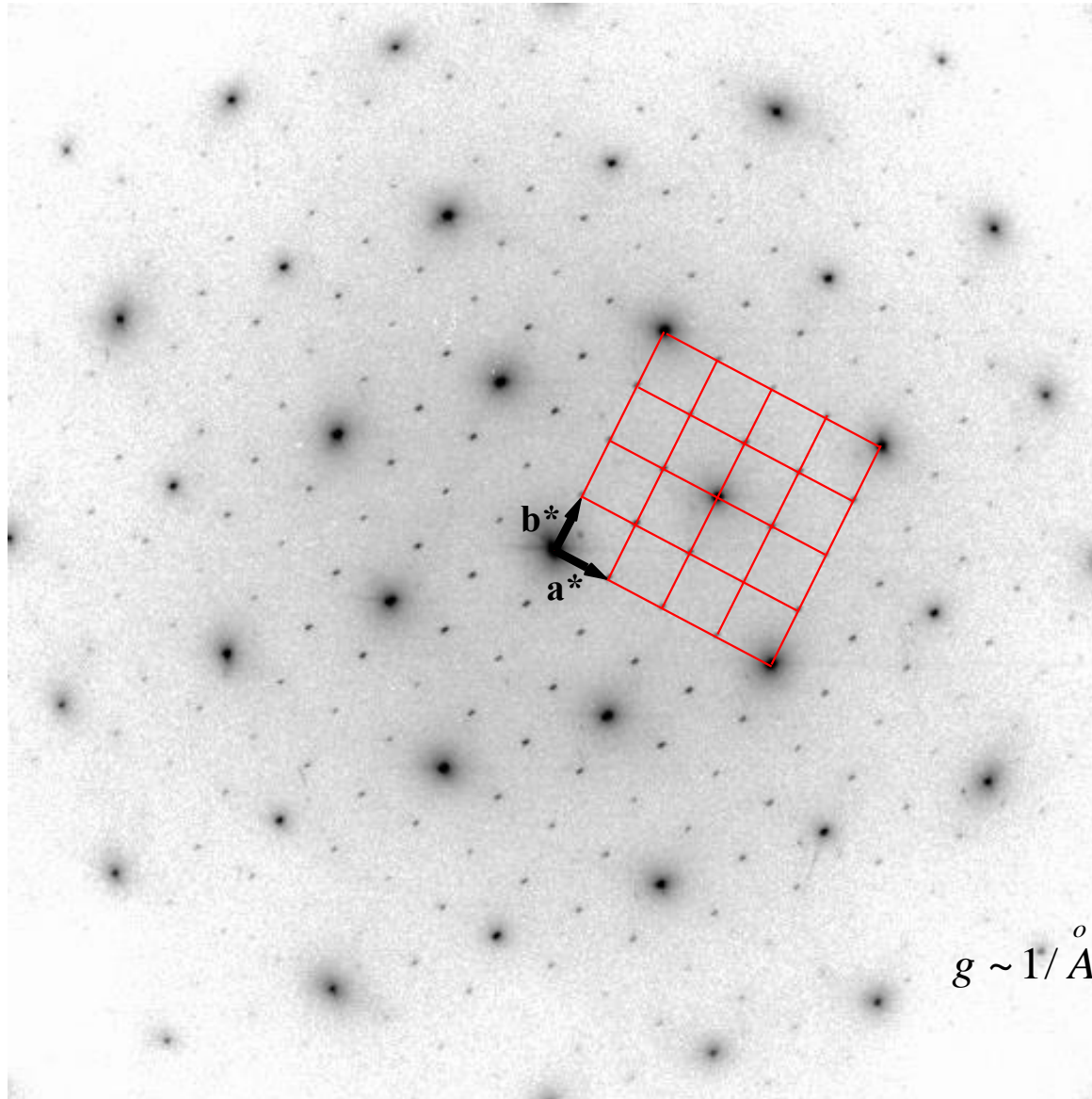
Ewald's sphere

The Ewald's sphere is a geometrical construction for interpreting diffraction patterns. When a beam hits a crystal, Ewald's sphere shows which sets of planes are at (or close to) the Bragg angle for diffraction to occur.



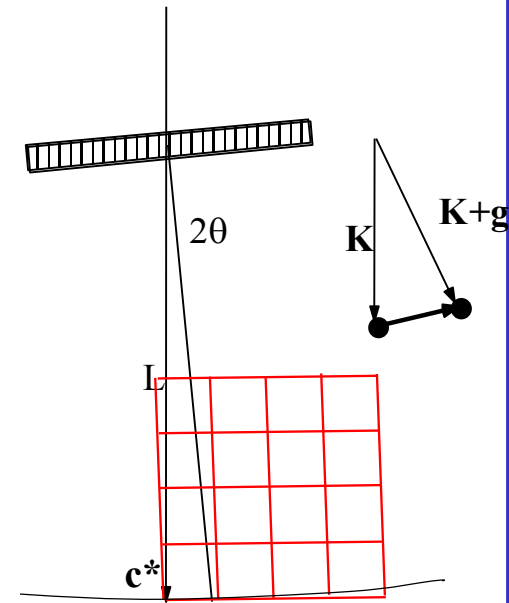
In electron diffraction, we see many diffraction spots at the same time because the Ewald's sphere is very flat (λ is small and k is large). For thin samples the reciprocal lattice points are stretched (relrods) and we see even more diffraction spots.

Crystal Diffraction Pattern and The Reciprocal Lattice



$$g \sim 1/\text{\AA},$$

$$\lambda \sim 0.025 \text{\AA}, \quad \theta \sim 12.5 \text{ mrad}$$



Bragg's Law

$$\sin \theta_B = \frac{g\lambda}{2}$$

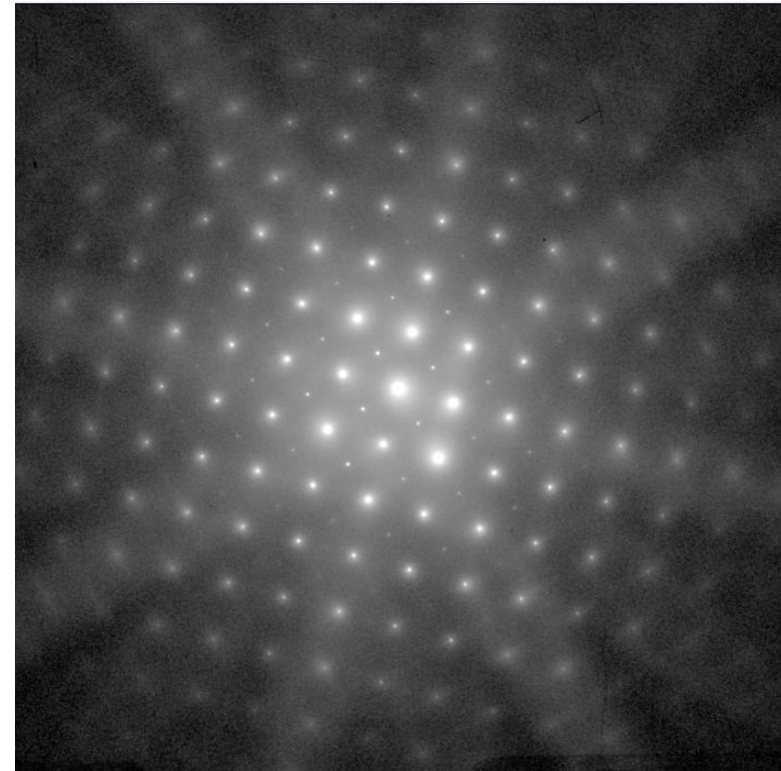
Kikuchi Lines

We see Kikuchi lines because:

1. The specimen is thick enough (~50 nm or above, 200 kV)
2. Electrons are scattered off Bragg angles in all directions (because of inelastic scattering)
3. These electrons are then Bragg diffracted by lattice planes

Some facts:

1. The electron energy loss is small (most less a few tens of eV) and electrons have similar wavelength as the incident beam
2. Most electrons travels in directions close to the incident beam (forward direction)
3. Kikuchi described this in 1928 before invention of TEM



SrTiO₃, 200kV

Structure factor

A structure factor is a measure of the amplitude scattered by a unit cell of a crystal structure
or a Fourier transform of the projected potential of the scattering object ..

$V(\mathbf{r})$ is the total ground state potential (crystal potential) seen by the beam electrons.

V_g are the Fourier components, $V(\vec{r}) = \sum_g V_g \cdot e^{2\pi i \vec{g} \cdot \vec{r}}$ given by

$$V_g = \frac{F_{hkl}}{\Omega} = \frac{1}{\Omega} \sum_i f_i(s) \cdot e^{-2\pi i \vec{g} \cdot \vec{r}_i} \quad \text{where } f_i \text{ is the electron atomic scattering factor for atom } i, \Omega \text{ is volume, } s = \sin\theta/\lambda$$

In electron diffraction, we usually refer to U_g (in \AA^{-2}) as the structure factor

$$U_g = \frac{2m|e|}{h^2} V_g$$

Electron versus X-ray diffraction

Advantages:

- smaller area (probe can be less than unit cell)
- strong dynamical interactions - structure factor phase info generally available
- strong scattering at low scattering angles

$$f^{el} \propto \frac{Z - f^X}{s^2} \quad s = \frac{\sin \theta}{\lambda}$$

- sensitive to details in the electron bonding distribution

Structure factor amplitudes - comparable to best X-ray results (Pendellösung)

Structure factor phases -20-50 times better than best X-ray results

Limitations:

Not as established as X-ray methods

Computational complicated and time consuming

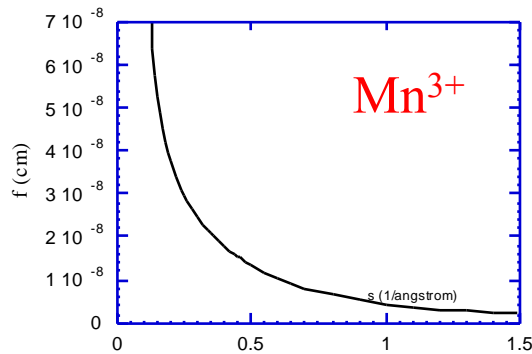
Refinements of small unit cell materials

Electrons, X-rays and Neutrons

Electrons

$$f(s) = \int v(\mathbf{r}) \exp(4\pi i \mathbf{s} \cdot \mathbf{r}) d\mathbf{r}$$

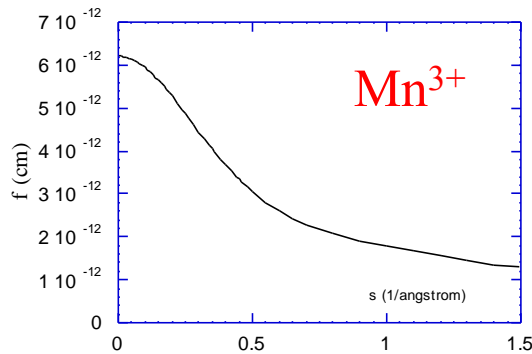
$$= 2.38 \times 10^{-10} \left(\frac{\lambda}{\sin \theta} \right)^2 (Z - f^x)$$



X-ray

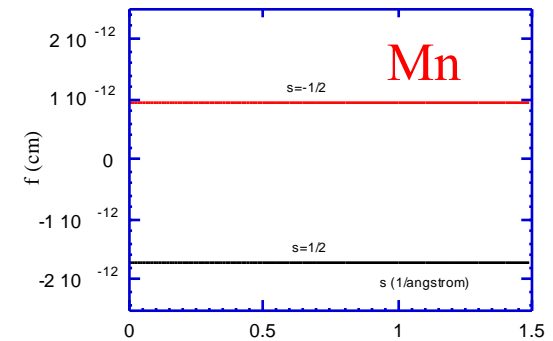
$$f^x(s) = \frac{e^2}{m_o c^2} \int \rho(\mathbf{r}) \exp(4\pi i \mathbf{s} \cdot \mathbf{r}) d\mathbf{r}$$

$$= 2.82 \times 10^{-13} f^x$$



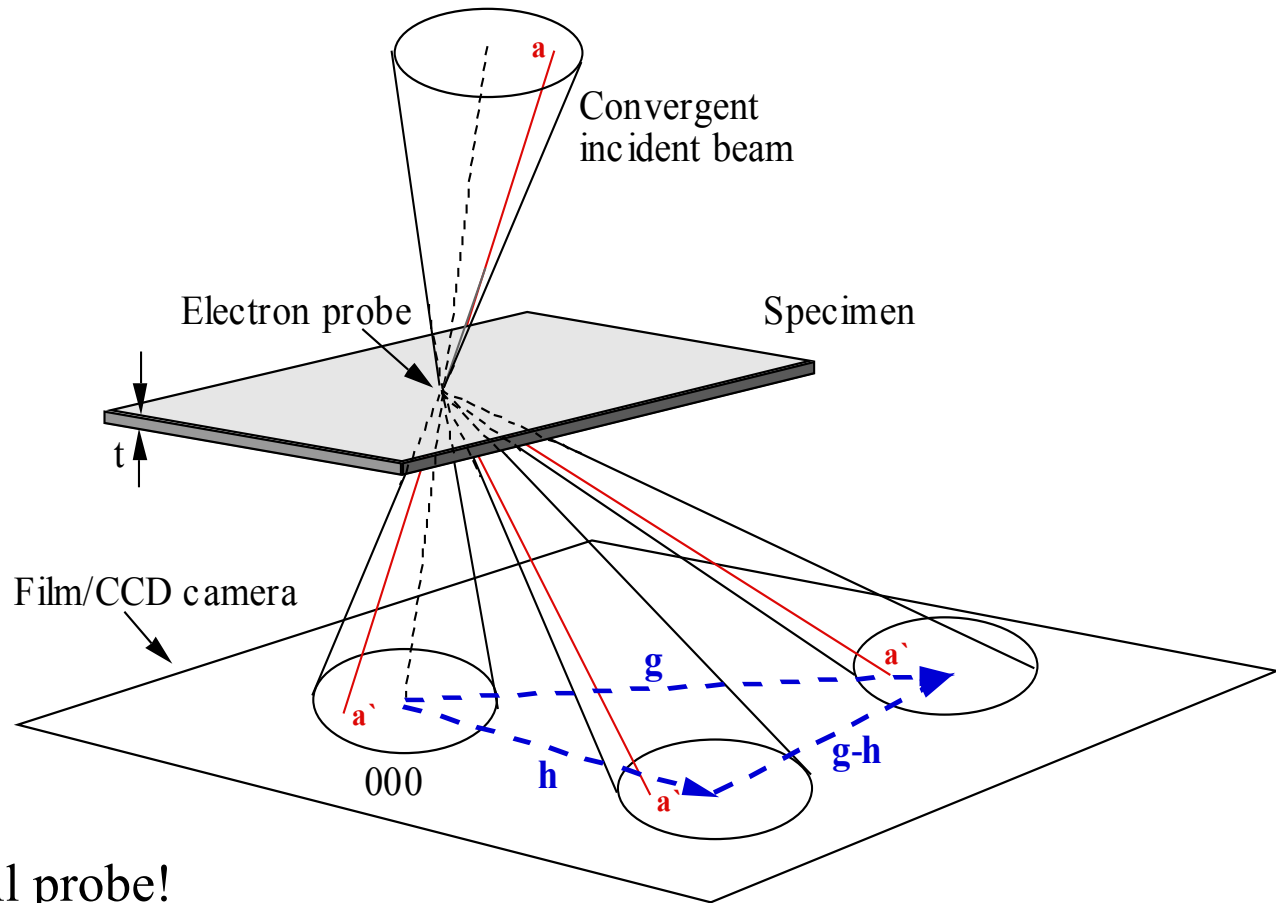
Neutrons

$$b = b_c + 2b_i [I(I+1)]^{1/2} \mathbf{s} \cdot \mathbf{I}$$



JM Zuo

Convergent beam electron diffraction

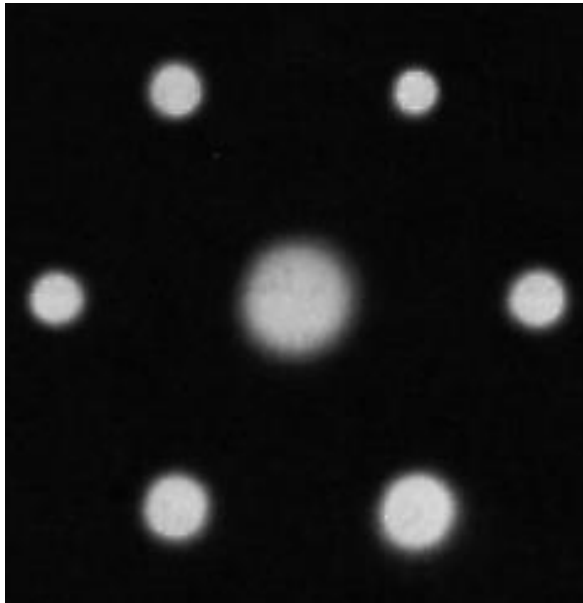


- Small probe!

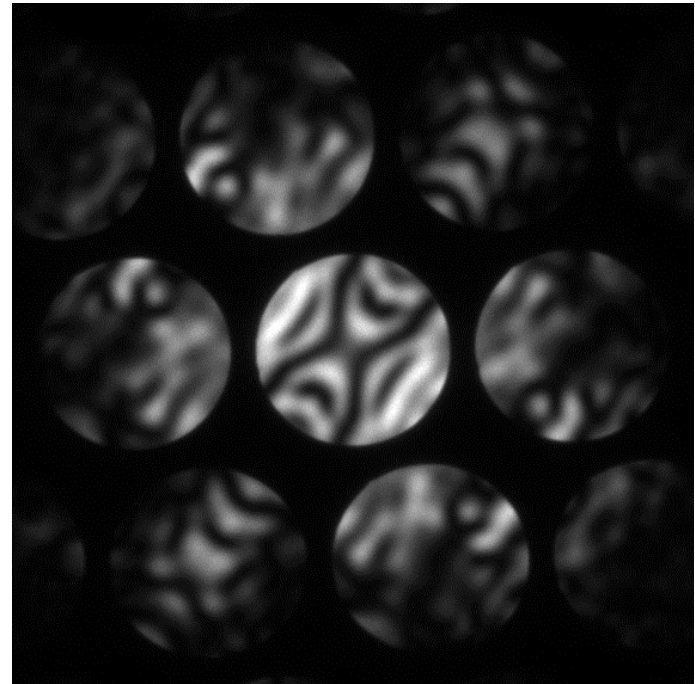
- Every point in the disc refers to one incident beam direction in the convergent beam and can be considered separately

Many independent spot patterns with slightly different beam orientation

CBED versus SAED

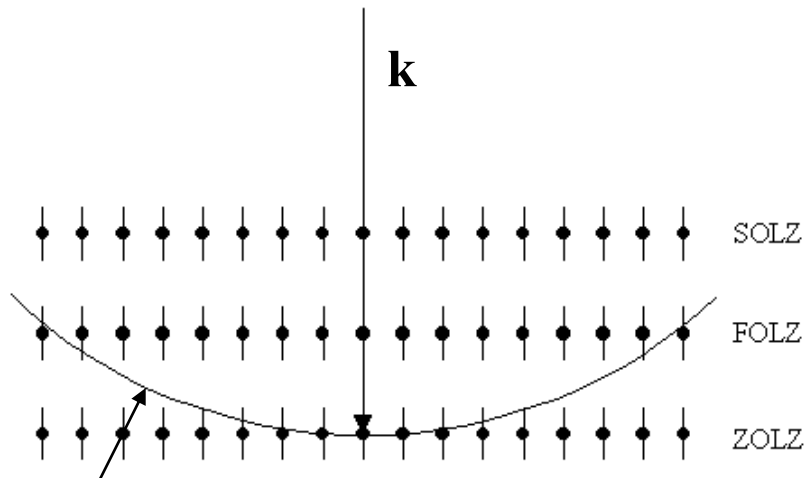


Spots of uniform intensity



Discs containing intensity variations

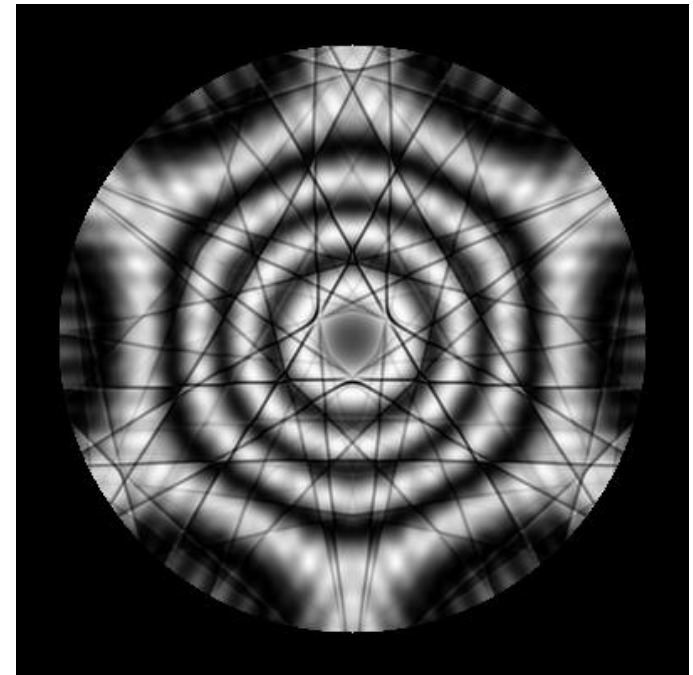
CBED and HOLZ line geometry



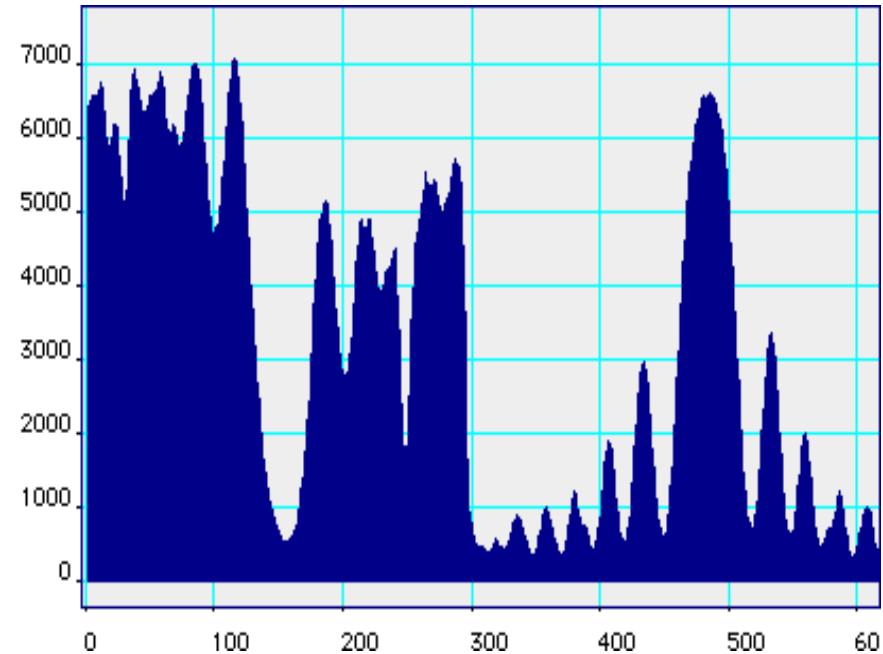
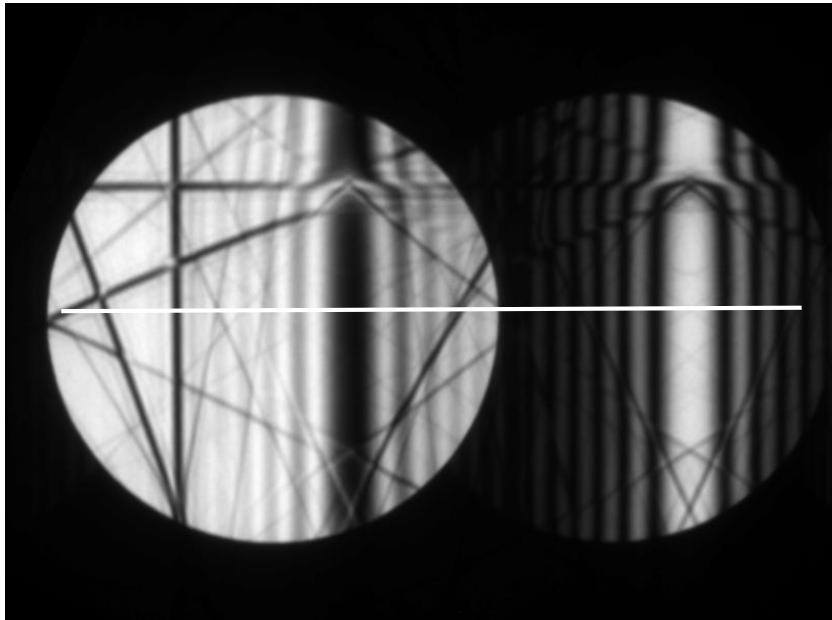
Ewald sphere

- ZOLZ reflections (discs)
- Sphere intersects other layers \Rightarrow HOLZ
- Zone-axis \Rightarrow HOLZ rings

- Electrons scatter from ZOLZ discs to form HOLZ ring
- HOLZ deficiency lines formed in ZOLZ discs
- Each line represents one diffracting plane

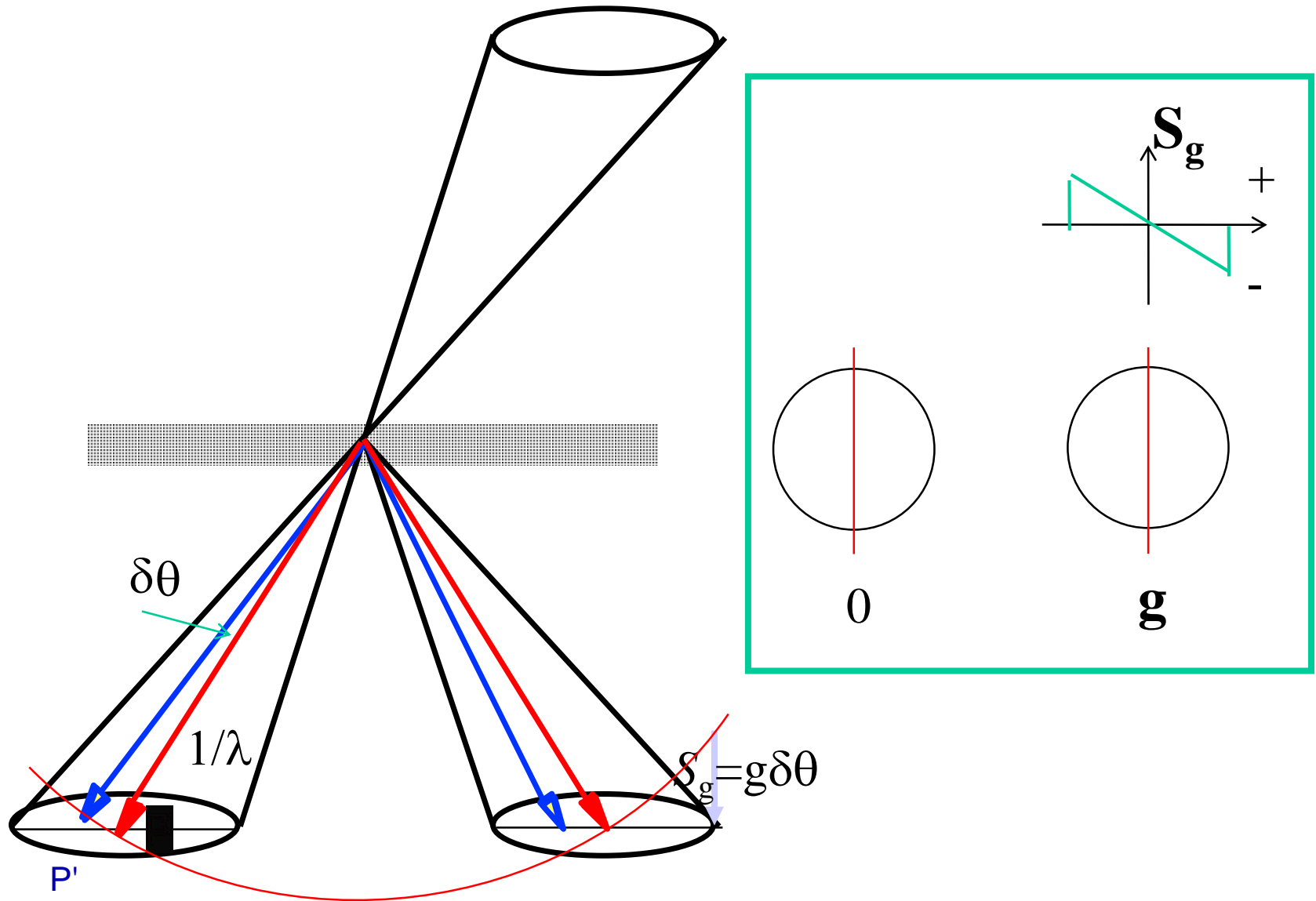


Why CBED?



- Single crystal diffraction due to small electron probe
- Mapping diffraction intensity as function of incident beam direction
- Same thickness, rocking curves
- Accurate measurements

Deviation from the Bragg Condition



Outline

- **Introduction to electron diffraction**
 - Basics in diffraction
 - Electron versus X-ray diffraction
 - SAED → CBED; geometry of CBED
- **Kinematic & dynamic (many beam) simulations**
 - Kinematic diffraction
 - Precession method: Pseudo-kinematic diffraction
 - Dynamical theory; two beam case
- **Experimental considerations**
 - Inelastic scattering, energy filtering
- **Refinement from CBED intensities**
 - Structure factors U_g and their relation to charge density
 - Refining low order U_g using dynamic diffraction intensities
- **Solving structures?**
- **'New' trends**
 - SPED, Scanning CBED, Coherent diffraction - Ptychography

CBED geometry

Center of Zero Disk

\vec{K}_t With origin at the zone axis center

Reflections

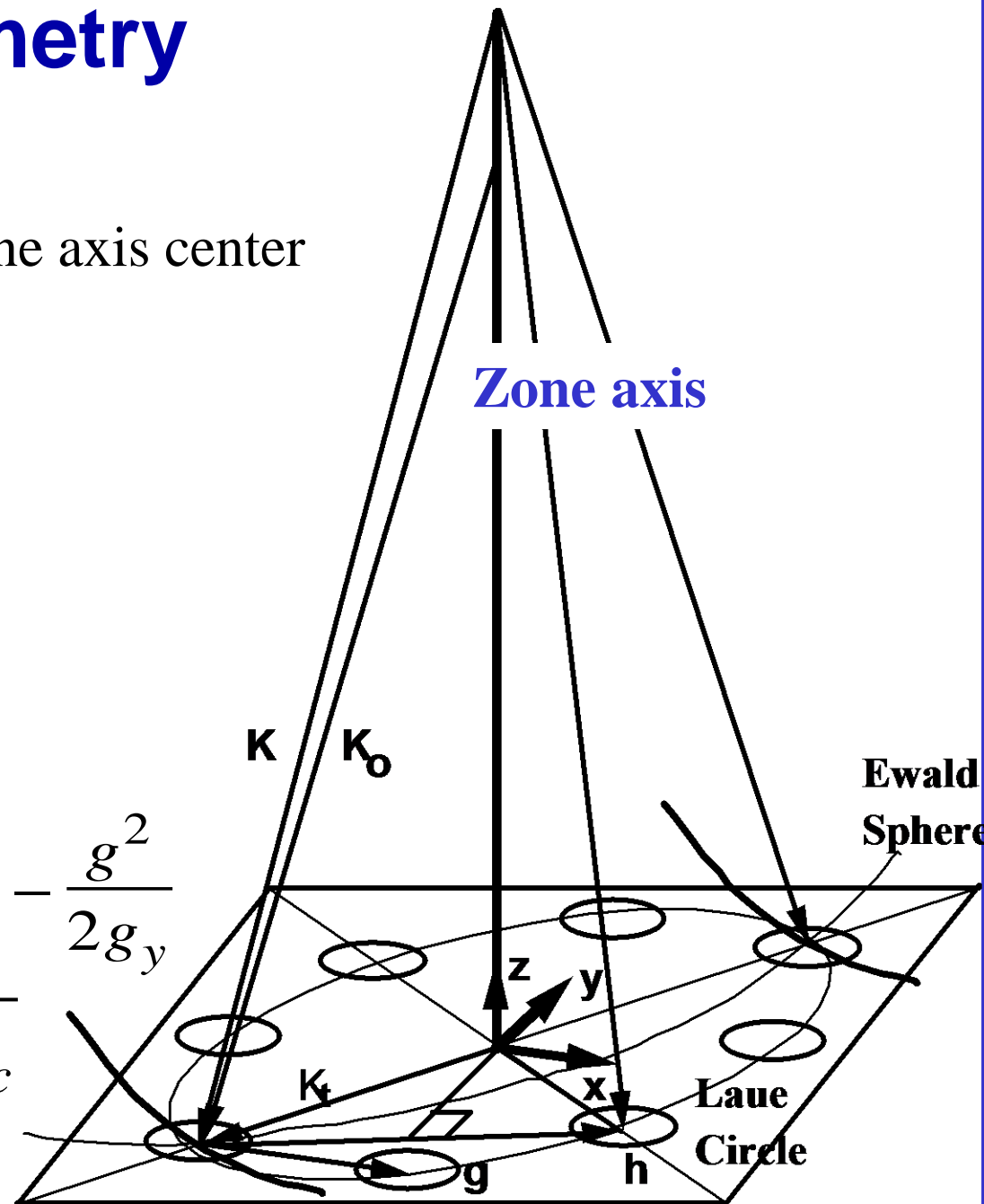
$$\vec{K}' = \vec{K}_t + \vec{g}$$

Lines

$$K^2 - (\vec{\mathbf{K}} + \vec{\mathbf{g}})^2 = 0$$

$$K_y = -\frac{g_x}{g_y} K_x + \frac{g_z}{g_y} K_z - \frac{g^2}{2g_y}$$

$$K_z \approx \sqrt{K^2 - K_{xc}^2 - K_{yc}^2}$$



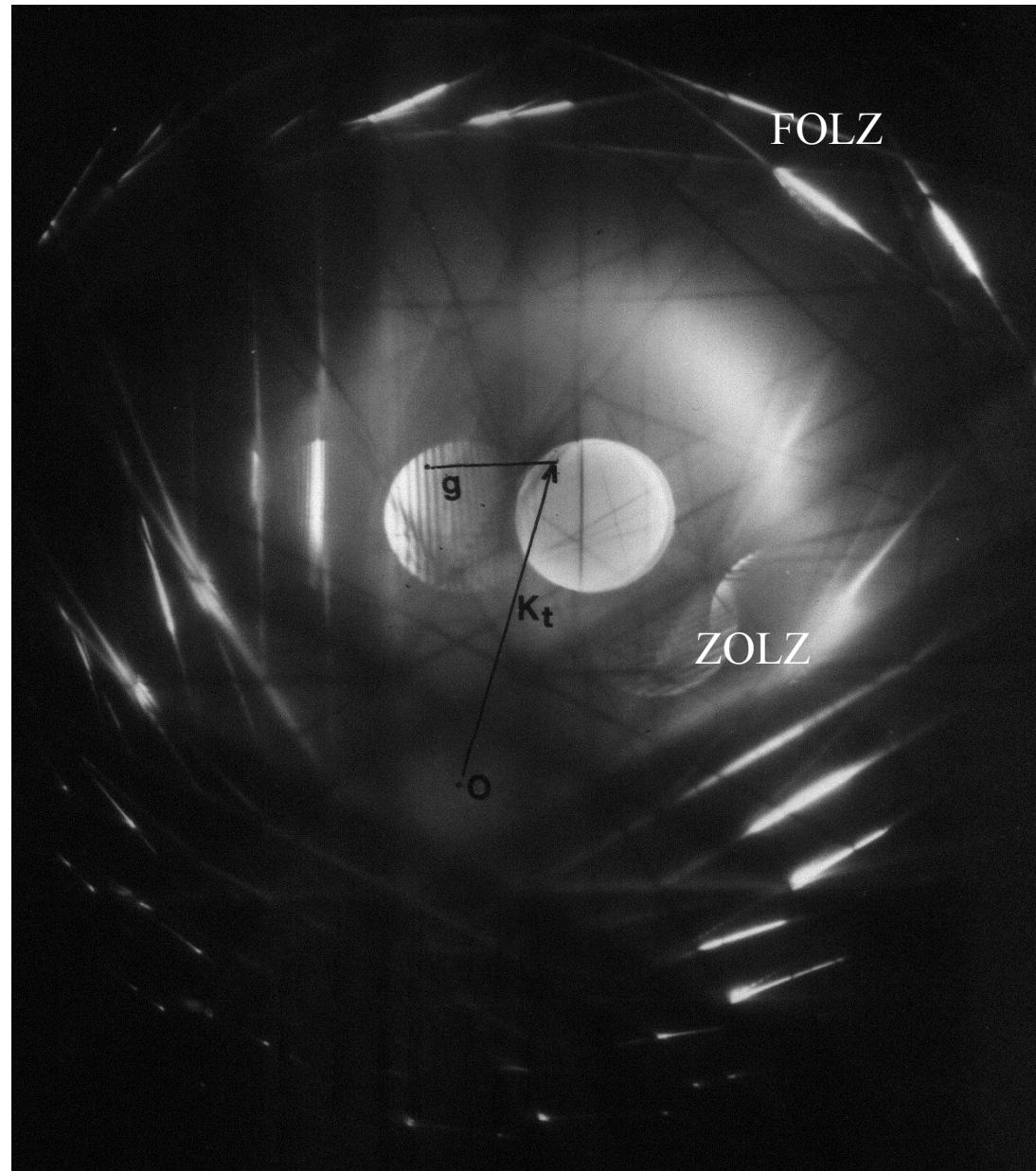
Simulations

Kinematical:

- Orientation
- Phase identification
- Crystal Lattice
- HV
- Structure (under favorable conditions!)

Dynamical:

- Thickness
- Polarity
- Atomic Structure
- Crystal Lattice
- Bonding



Kinematical theory of intensities

Electrons interact with matter through Coulomb potential

$$\nabla^2 V(\vec{r}) = -\frac{e[Z\delta(\vec{r}) - \rho(\vec{r})]}{\epsilon_o} \quad (U = 2meV / h^2)$$

Electron wave function is a plane wave (parallel beam): $\phi_o \approx \exp(2\pi i \vec{k}_o \cdot \vec{r})$

Scattering by a weak potential is given by the first-order Born approximation:

$$\phi_s = \frac{2\pi me}{h^2} \int \frac{V(\vec{r}')}{|\vec{r} - \vec{r}'|} e^{2\pi i \vec{k} \cdot (\vec{r} - \vec{r}')} e^{2\pi i \vec{k}_o \cdot \vec{r}'} d\vec{r}' \approx \frac{2\pi me}{h^2} \frac{e^{2\pi i \vec{k}_o \cdot \vec{r}}}{r} \int V(\vec{r}') e^{2\pi i (\vec{k} - \vec{k}_o) \cdot \vec{r}'} d\vec{r}'$$

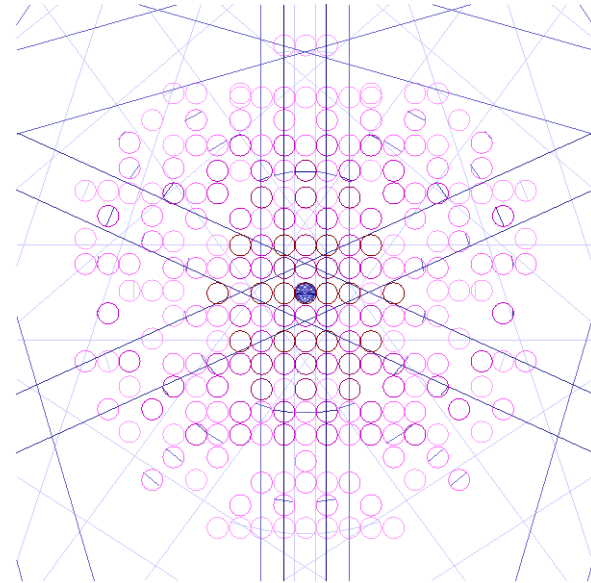
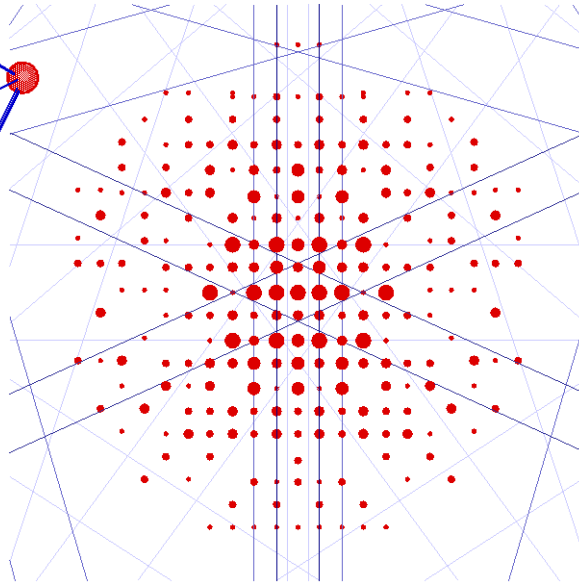
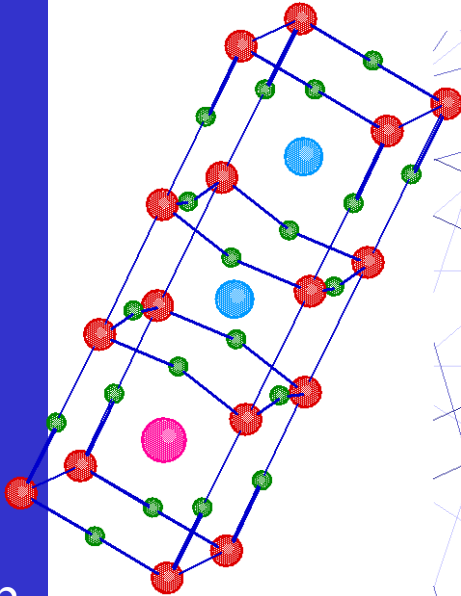
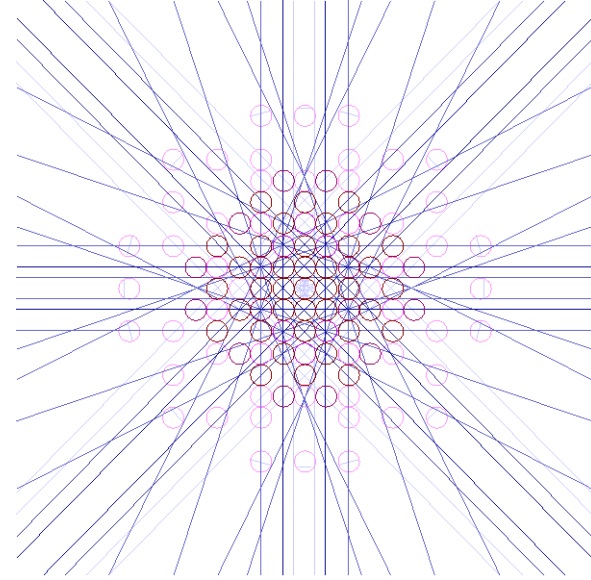
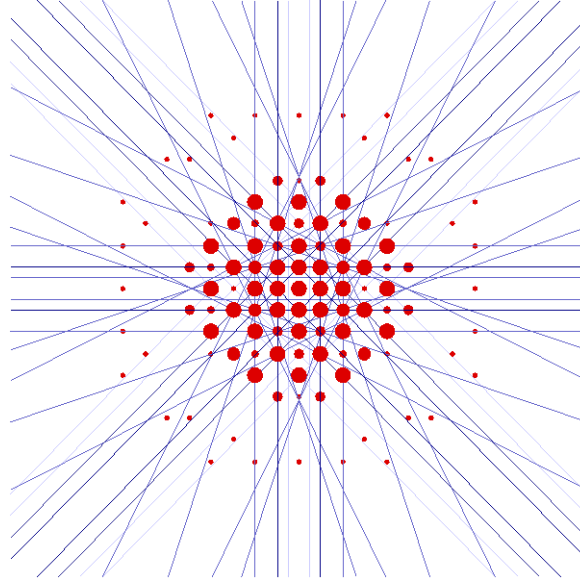
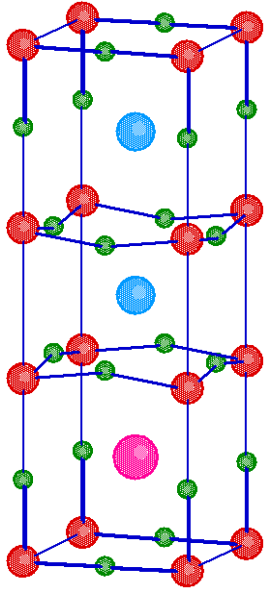
Scattered intensity depends only on the magnitude of the structure factors

$$I_g = |\phi_s|^2 \propto |U_g|^2 S(S_g)$$

(Shape factor S is the same for all reflections)

Phase information lost!

Electron diffraction simulation, kinematic



X-tilt = 26.5°

Precession method

- precess the focused incident beam at a constant angle around a zone axis in combination with a similar precession of the beam below the specimen
- reflections swept successively through the Ewald sphere
- integrated intensities recorded as uniform discs (Fig. 1a).
- the diffraction conditions during the precession movement can be visualised by the equivalent rotation of the Laue circle about the central spot (Fig. 1b).
- integration reduce sensitivity to thickness - multiple beam dynamical effects are less than in the SAED patterns because the beam is off the zone axis.

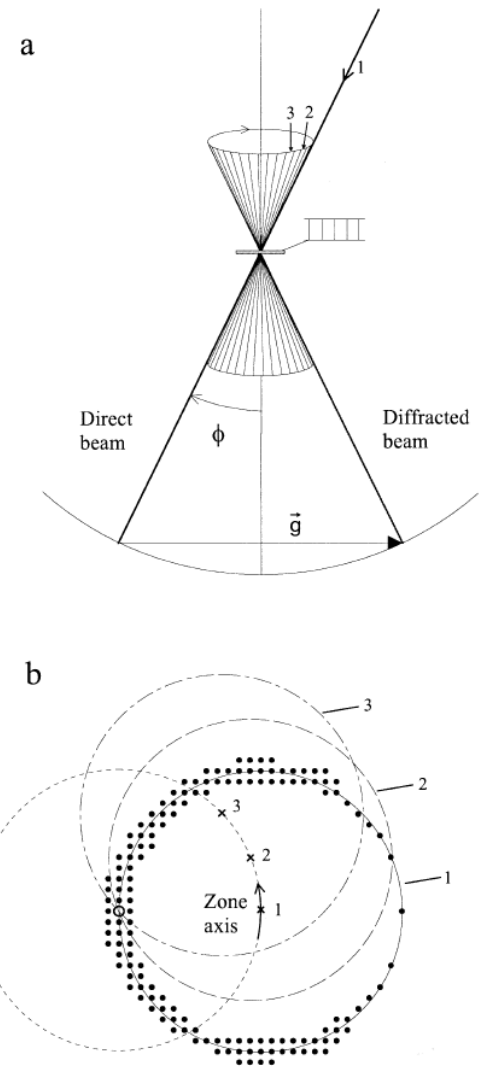


Fig. 1. The precession technique devised by Vincent and Midgley [8]. (a) The incident beam is precessed at a constant angle (ϕ) around the optic axis in combination with a similar precession of the beam below the objective lens. The probe size is about $0.1 \mu\text{m}$. (b) During precession, the Laue circle rotates about the zero beam and sweeps the zero Laue zone.

Precession method - Pseudo-kinematic diffraction

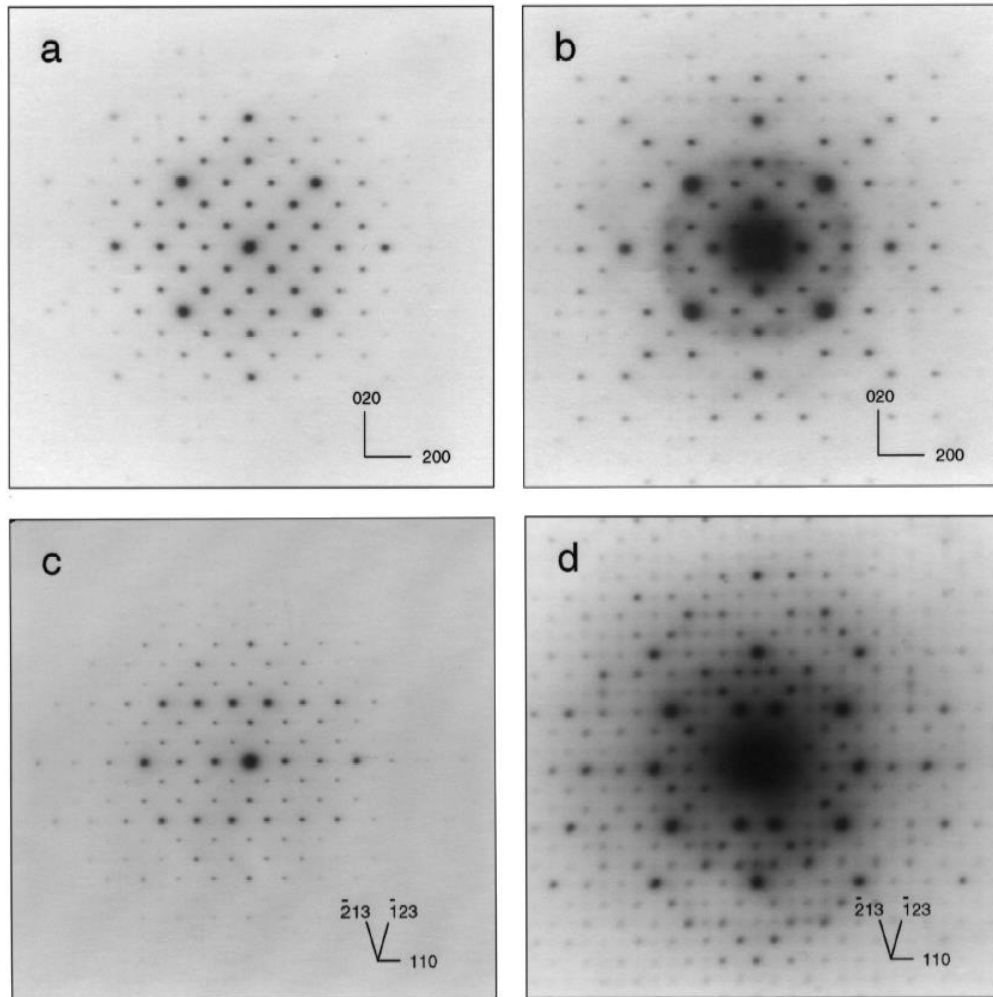


Fig. 2. Electron diffraction patterns of the intermetallic alloy phase Al_3Fe . (a) $[0\ 0\ 1]$ projection, SAD pattern, (b) $[0\ 0\ 1]$ projection, precessed pattern ($\phi = 2.35^\circ$), (c) $[1\ 1\ 1]$ projection, SAD pattern and (d) $[1\ 1\ 1]$ projection, precessed pattern ($\phi = 2.45^\circ$).

Berg, Hansen, Midgley and Gjønnes
Ultramicroscopy, 74, 147, 1998.

Dynamic diffraction theory

(Bloch wave method!)

Start out with the Schrödinger equation

$$\frac{-\hbar^2}{8\pi^2m} \nabla^2 \Psi(\mathbf{r}) - |e|V(\mathbf{r}) \Psi(\mathbf{r}) = E_o \Psi(\mathbf{r})$$

Set in Bloch waves

excitation amplitude of i'th Bloch wave

Bloch wave coefficient

$$\Psi(\mathbf{r}) = \sum_i c_i \exp(2\pi i \mathbf{k}^i \cdot \mathbf{r}) \sum_g C_g^i \exp(2\pi i \mathbf{g} \cdot \mathbf{r})$$

and Fourier expansion of potential

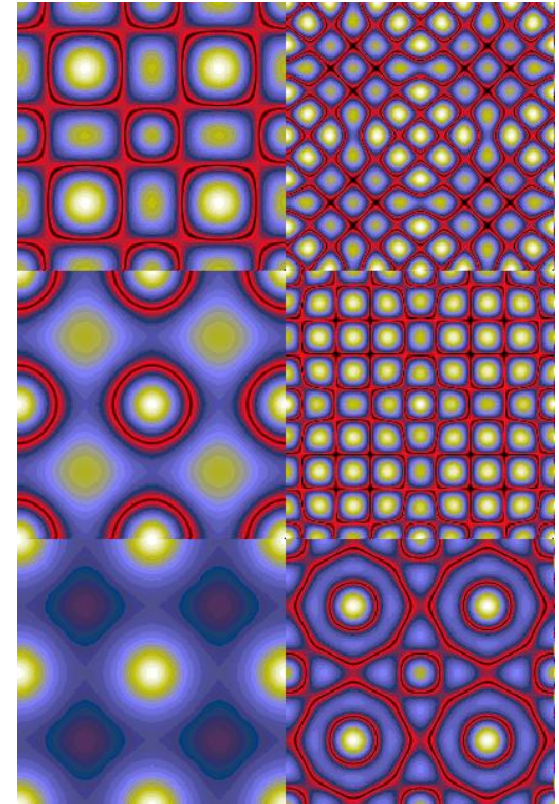
$$U(\mathbf{r}) = \frac{2m|e|}{h^2} V(\mathbf{r}) = \sum_g U_g \exp(2\pi i \mathbf{g} \cdot \mathbf{r})$$

and introduce

$$K^2 = \frac{2m|e|}{h^2} (E + V_0)$$

Then we get the fundamental equations

$$\left[K^2 - (\mathbf{k}^i + \mathbf{g})^2 \right] C_g^i + \sum_h U_{gh} C_h^i = 0$$



Bloch waves have the symmetry of the crystal - look like atomic states (1s, 2s, 2p, etc.)

Note:

The set of equations is exact only for an infinite number of beams –

The accuracy of the calculated intensities depends on the accuracy of the crystal potential used in the calculation. This is related to the number of Fourier components (g) included in the Fourier series representing the potential.

Including the Fourier component (or structure factor) will lead to the calculation of the diffracted intensity from the plane g .

In electron diffraction we use terms such as **‘incident beam’** and **‘diffracted beams’**, and the number of Fourier components is generally referred to as **‘the number of beams’** in the calculation.

More beams mean a more accurate scattering potential and, hence, a more accurate set of diffracted intensities. While many hundreds of beams may often be required to obtain a ‘perfect’ simulation, calculations using a few tens of beams are often sufficient for qualitative comparisons between theory and experiment.

Introducing the excitation error S_g and Anpassung γ , we get from the figure

$$|(\mathbf{k}^i + \mathbf{g})|^2 = [K + (\gamma^i - S_g)]^2$$

$$[K^2 - (\mathbf{k}^i + \mathbf{g})^2] \cong 2K(S_g - \gamma^i)$$

We have assumed that γ and S_g both have direction parallel to \mathbf{n}

The new fundamental equations

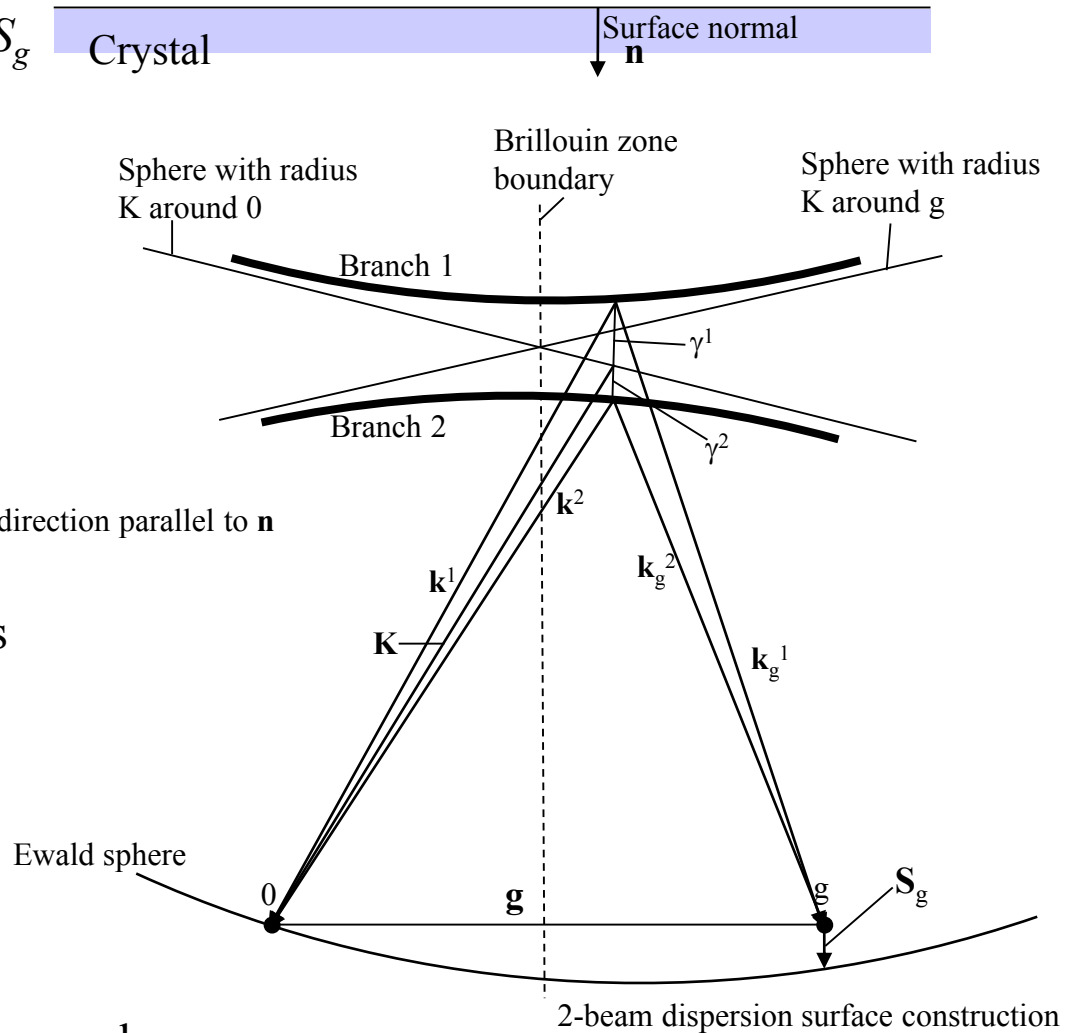
$$2K S_g C_g^i + \sum_{h \neq g} U_{gh} C_h^i = 2K \gamma^i C_g^i$$

-scattering matrix A on left side!

These equations represent an Eigenvalue problem with Bloch wave eigenvectors C_g^i and eigenvalues γ^i .

Intensity given by

$$I_g(x, y) = |\psi_g(\mathbf{r})|^2 = \left| \sum_{i=1}^N c_i(x, y) C_g^i(x, y) \exp[2\pi i \gamma^i(x, y) t] \right|^2$$



Bloch wave simulations

$$I_g(x, y) = \left| \Psi_g(\mathbf{r}) \right|^2 = \left| \sum_{i=1}^N c_i(x, y) C_g^i(x, y) \exp[2\pi i \gamma^i(x, y) t] \right|^2$$

Input:

Crystal parameters (unit cell, atom positions, space group)

Microscope parameters (high voltage, convergence angle)

Diffraction condition (zone axis, surface normal, k_t , x-axis)

- (1) Select beams to diagonalise (strong) $i = 1, \dots, N$ and include by perturbation (weak) based on distance to Ewald sphere and strength
- (2) U_g is calculated using the atomic potential model and Einstein model for absorption
- (4) Solve by matrix diagonalisation for each point in the CBED zero disk; weak beams treated by perturbation
- (4) Calculate c_i using the boundary condition

Interaction Potentials

Electron interaction potential has three components: the first is the real, crystal, Coulomb potential and the second and third are the real and imaginary part of the absorption potential.

$$U_g = U_g^C + U_g'' + iU_g'$$

Where $U_g = 2m|e|V_g / h^2$ and

$$V_g^C = \int d^3\vec{r} \exp(2\pi i\vec{g} \cdot \vec{r}) \langle V(\vec{r}) \rangle = \frac{|e|}{4\pi\epsilon_0 g^2} (Z_g - F_g)$$

With $Z_g = \sum_i Z_i T(\vec{g}) \exp(2\pi i\vec{g} \cdot \vec{r})$

and F_g is the averaged X-ray structure factor.

Beam selection criteria

- Too many give long computation time and numerical instabilities
- Too few give decreased accuracy

Include beams \mathbf{g}

- up to a max excitation error $|2KS_g| \leq |2KS_g|_{\max}$ (shell around Ewalds sphere)
- up to a max g-vector $|g| \leq g_{\max}$ (sphere around origin)
- inside sphere and outside shell with $\left| \frac{U_g}{2KS_g} \right| \geq \left| \frac{U_g}{2KS_g} \right|_{\min}$

Out of these, decide which to diagonalise (\mathbf{g} , strong)
and treat by Bethe perturbation (\mathbf{h} , weak)

Beam \mathbf{h} is considered weak if

$$|2KS_h| \geq |2KS_h|_{\min}$$

or
$$\omega = \left| \frac{KS_h}{U_h} \right| \geq \omega_{\max}$$

Zuo, JM. and Weickenmeier, AL,
Ultramicroscopy, 57, 375 (1995)
Birkeland C, Holmestad R, Marthinsen K, Høier R
Ultramicroscopy, 66, 89 (1996)

Two-beam case

In the two-beam theory, only two reciprocal lattice points (0 and \mathbf{g}) are considered. The fundamental equations can be solved exactly.

Intensity (no absorption) is given by

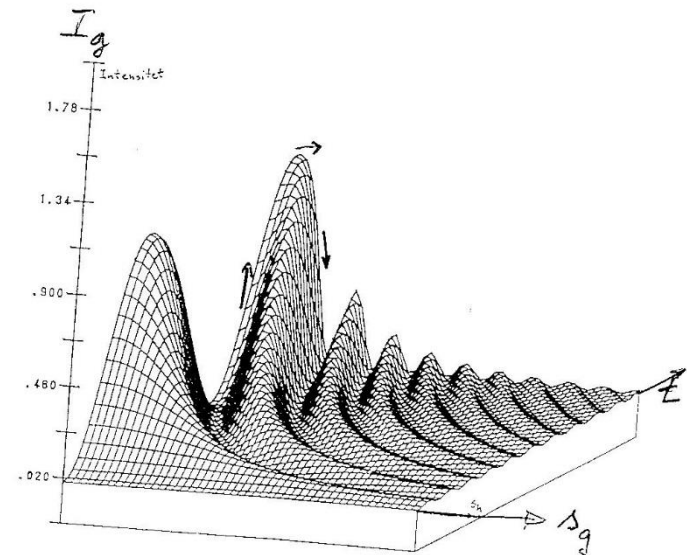
$$I_g = 1 - I_0 = \frac{|U_g|^2 \sin^2 \left(\frac{\pi t}{K} \sqrt{K^2 S_g^2 + |U_g|^2} \right)}{K^2 S_g^2 + |U_g|^2}$$

Introducing the extinction distance

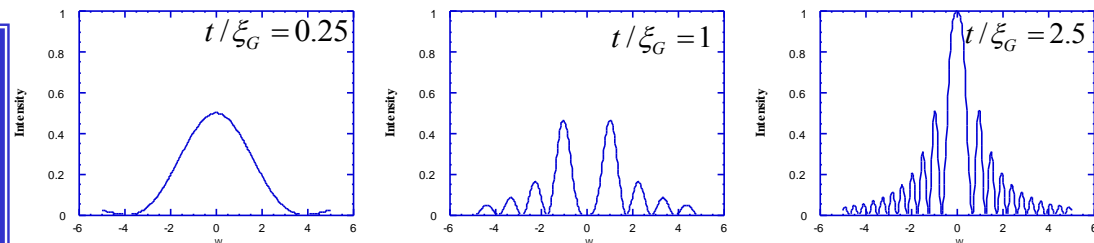
$$\xi_g = \frac{K}{|U_g|}$$

We get the expression

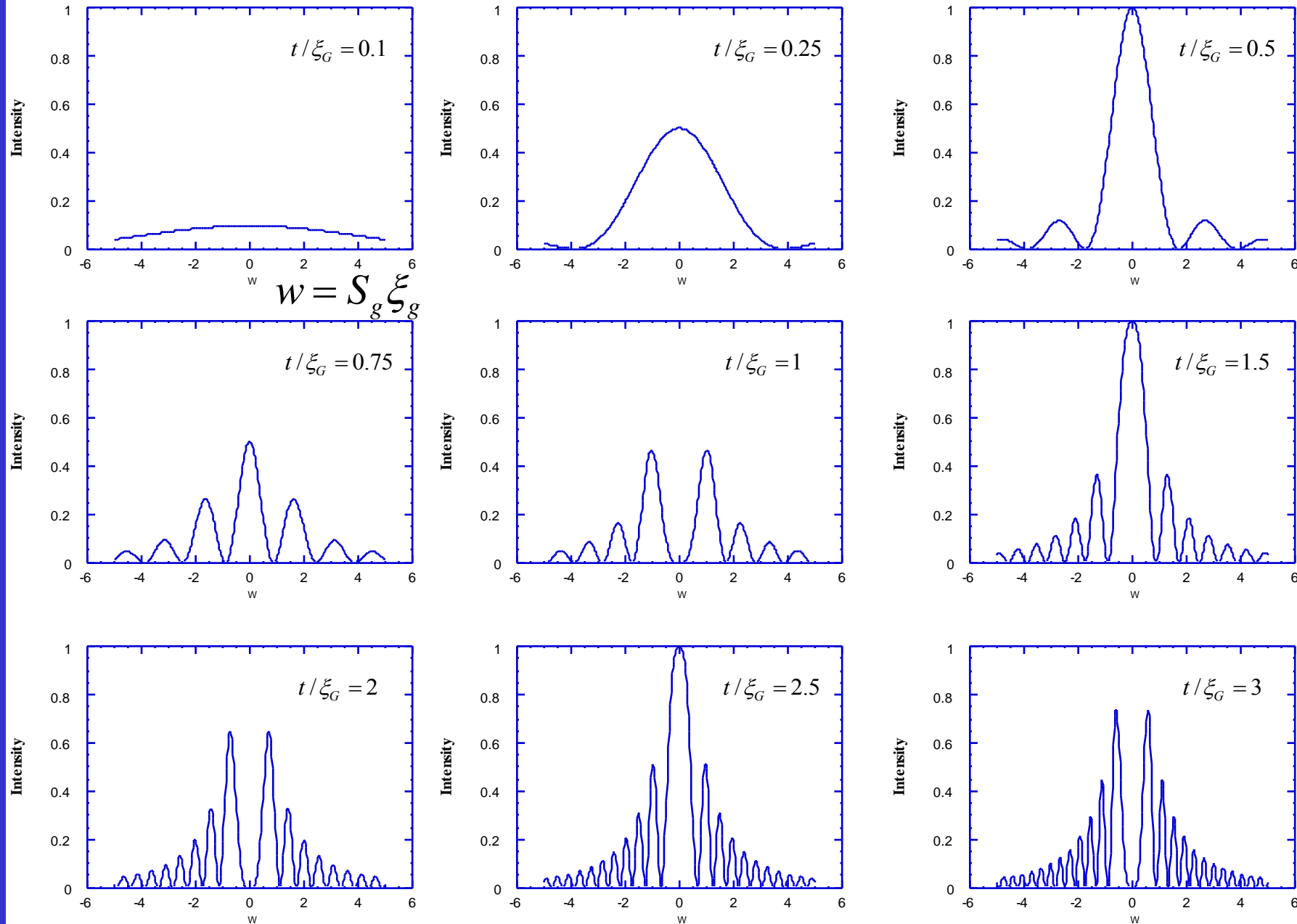
$$I_g = 1 - I_0 = \frac{\sin^2 \left(\pi t \sqrt{S_g^2 + \frac{1}{\xi_g^2}} \right)}{1 + S_g^2 \xi_g^2}$$



Two-beam rocking curves for different thicknesses:



Dynamic Diffraction: Two Beam Case



Thickness determination

The specimen is tilted to a two-beam condition, and we use the two-beam intensity to determine thickness

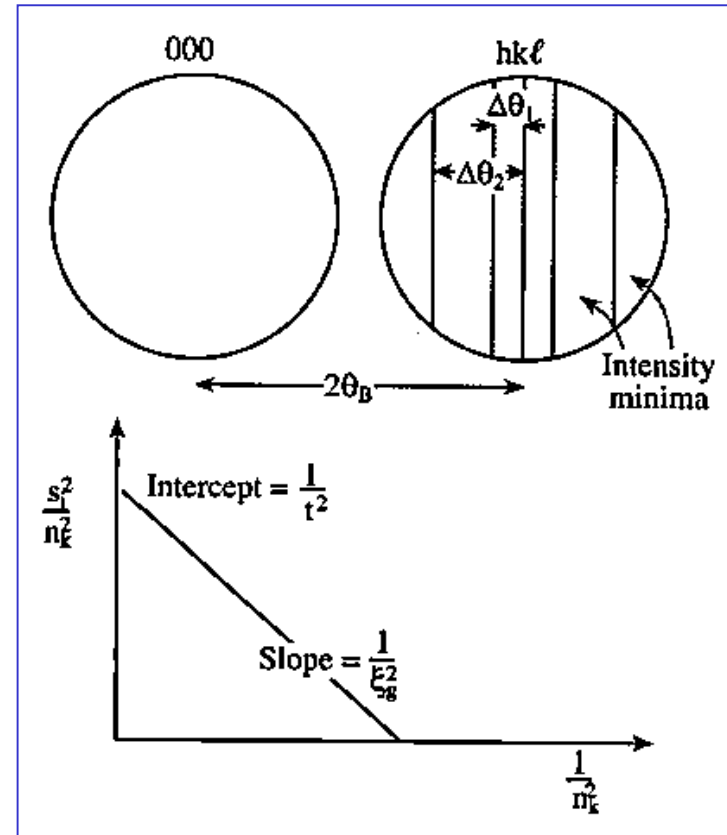
■ Plot

$$\left(\frac{s_i}{n_i}\right)^2 = -\frac{1}{(n_i \xi_g)^2} + \frac{1}{t^2}$$

where

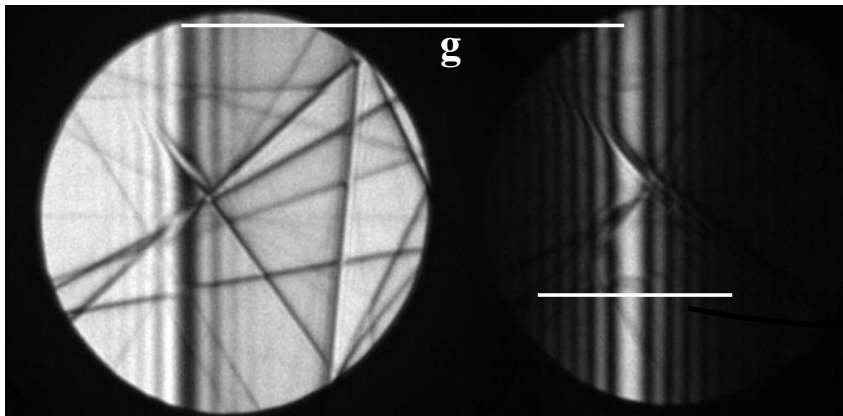
$$s_i = \frac{\lambda}{d^2} \frac{\Delta\theta_i}{2\theta_B}$$

d =planar spacing for reflection g
 l = electron wave length

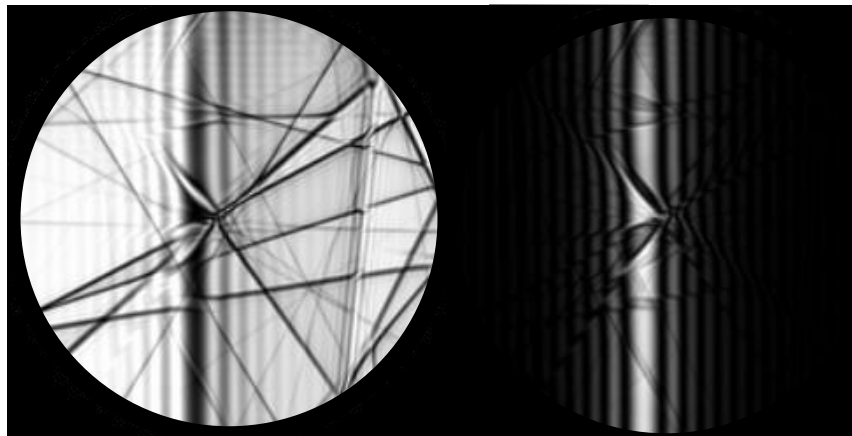
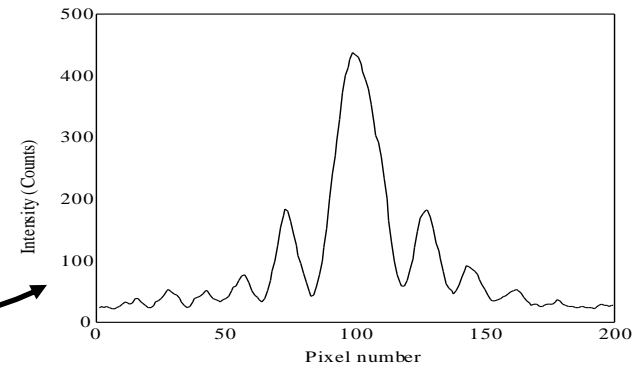


- Need to choose correct values for n

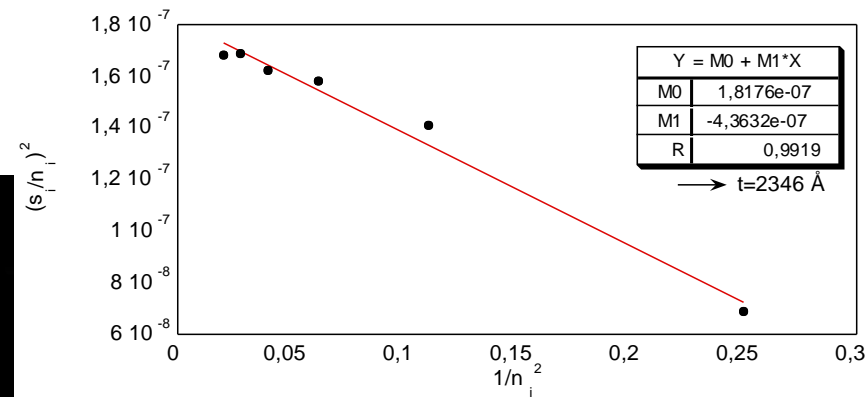
Example -thickness determination



(311) systematic row in CaF_2 .

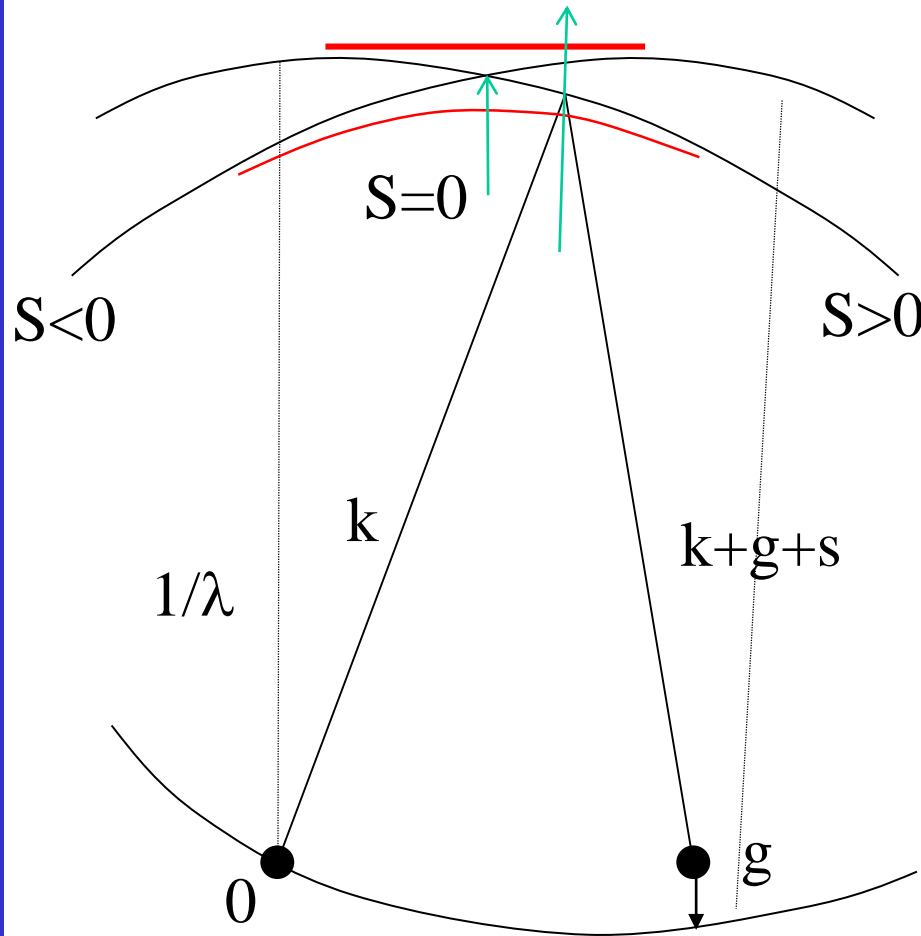


Simulation with thickness 2346 Å.



Plot of $(s_k^i/n_i)^2$ versus $(1/n_i)^2$ for $n_l=1$ gives thickness equal to 2346 Å (and $\xi_g=1514$ Å).

Dispersion Surface



$$\gamma^{1,2} = \left[s_g \mp \sqrt{s_g^2 + 1/\xi_g^2} \right] / 2$$

$S>0$, for large s

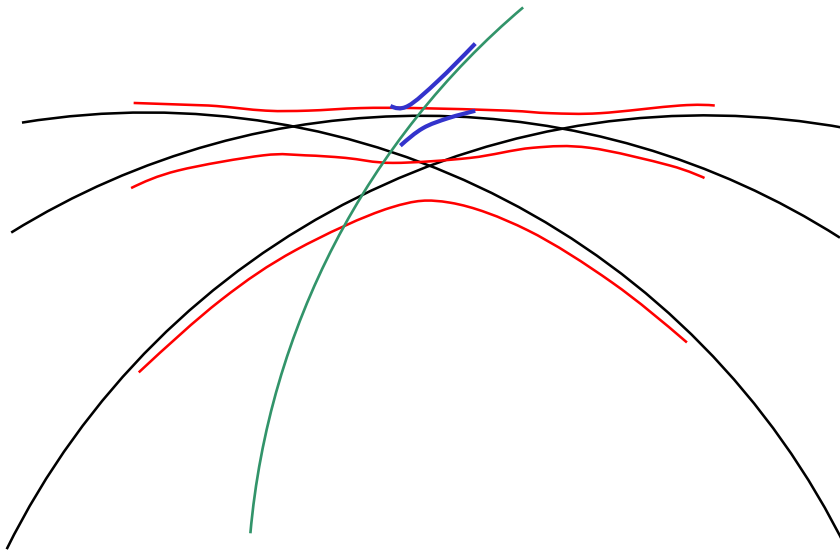
$$\gamma^1 \approx \left(S_g - S_g - \xi_g^2 / 2S_g \right) / 2$$

$$= -1 / \left(4S_g \xi_g^2 \right)$$

$$S=0 \quad \gamma^1 = -1 / 2\xi_g$$

➡ Electron wave vectors allowed in the crystal

Many Beam Case



HOLZ line position
determined by
intersection with the
dispersion surface!

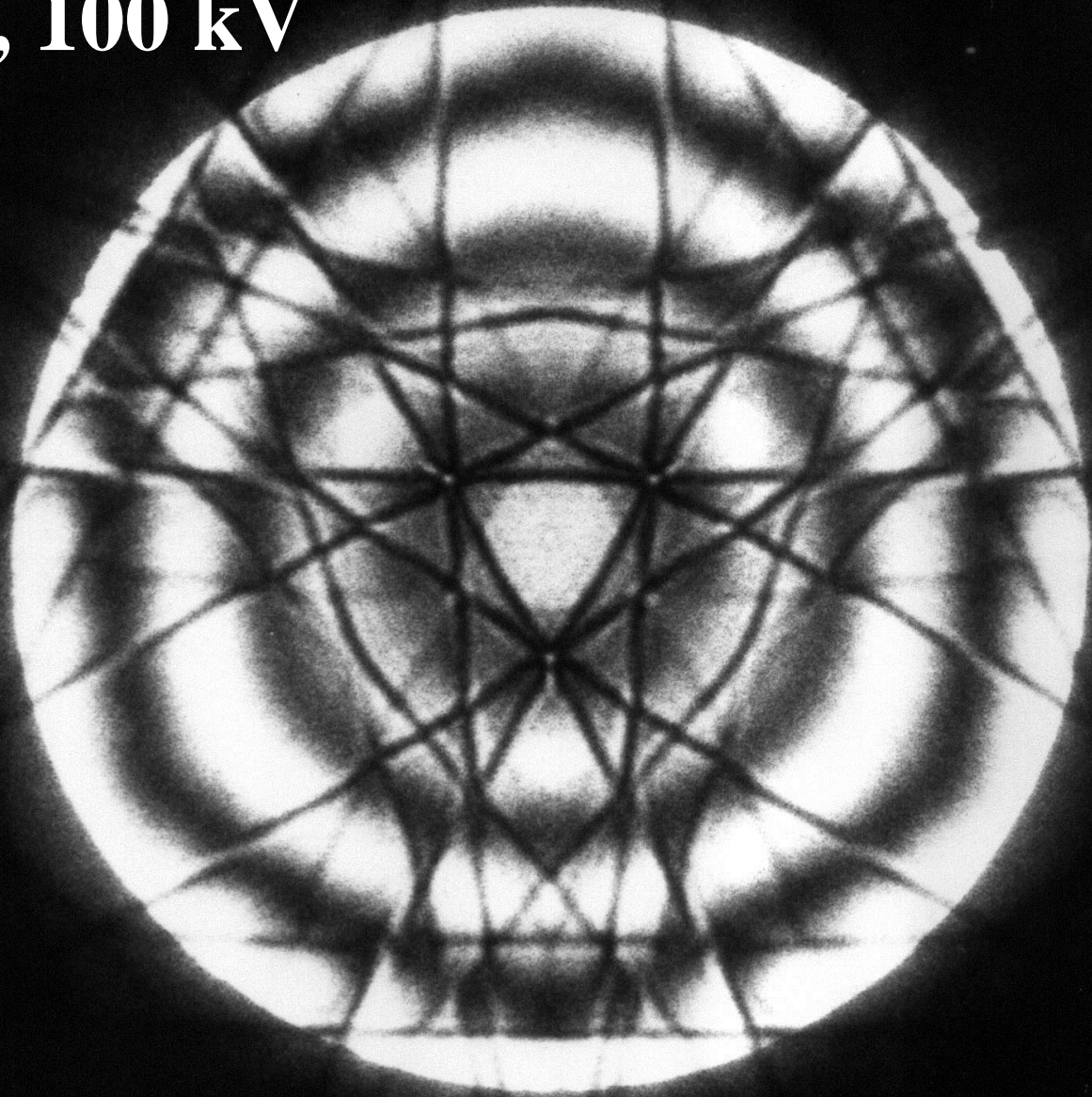
● h

● $-\frac{1}{2}$

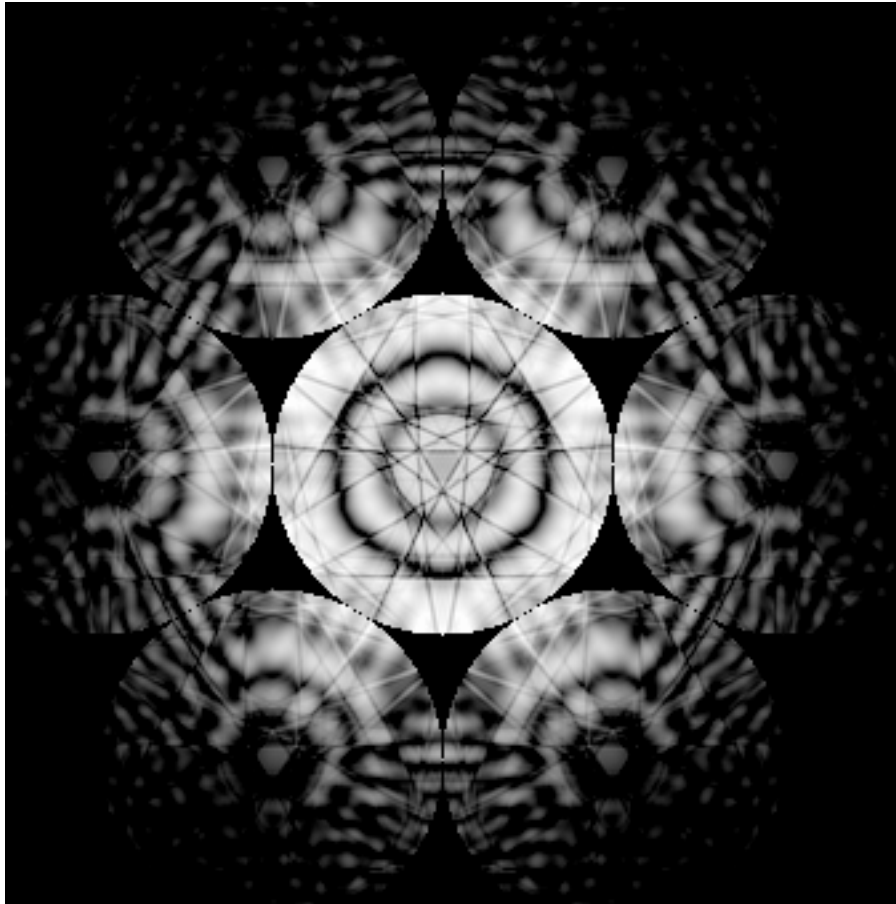
● 0

● $\frac{1}{2}$

Si [111], 100 kV



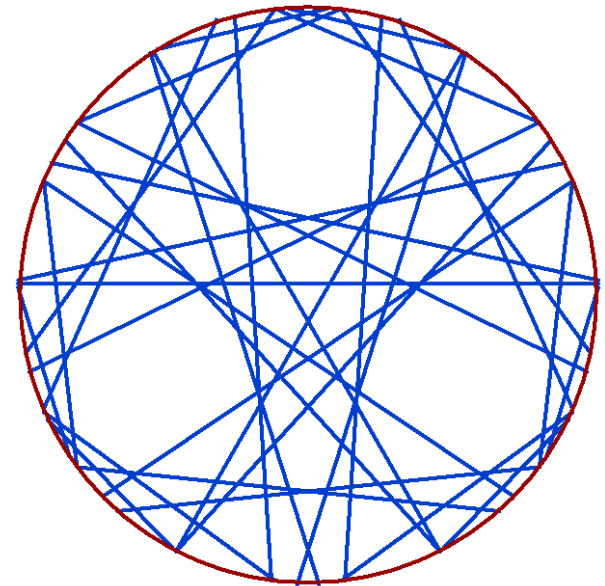
Kinematic versus Dynamic



Simulated, 100kV, Si[111], 160 beams

Kinematic Geometry:

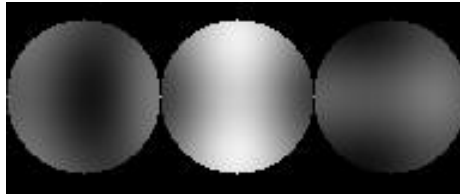
$$K^2 - (\mathbf{K} + \mathbf{g})^2 = 0$$



100 kV

GaN Polarity Determination

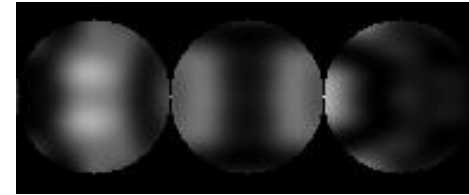
GaN [110], 300 kV



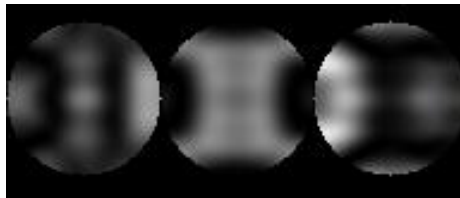
250 Å



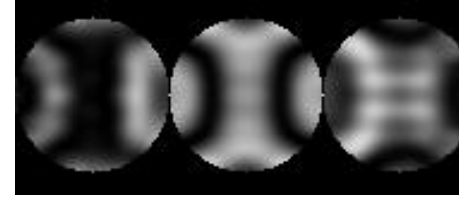
500 Å



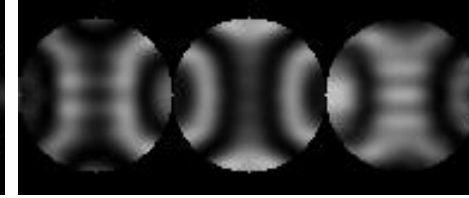
750 Å



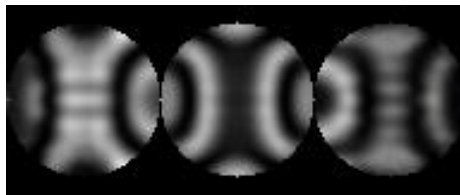
1000 Å



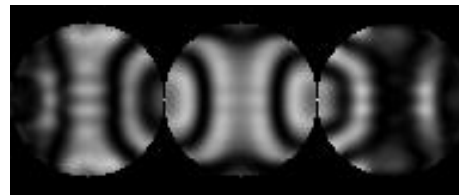
1250 Å



1500 Å



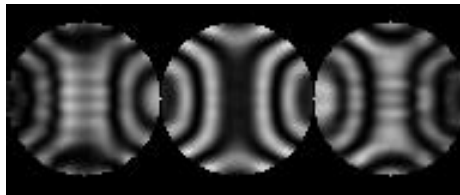
1750 Å



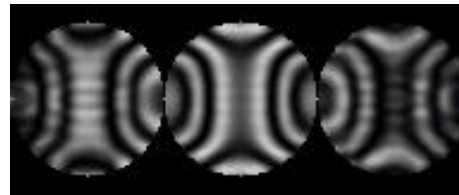
2000 Å



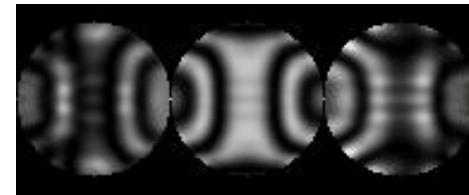
2250 Å



2500 Å



2750 Å



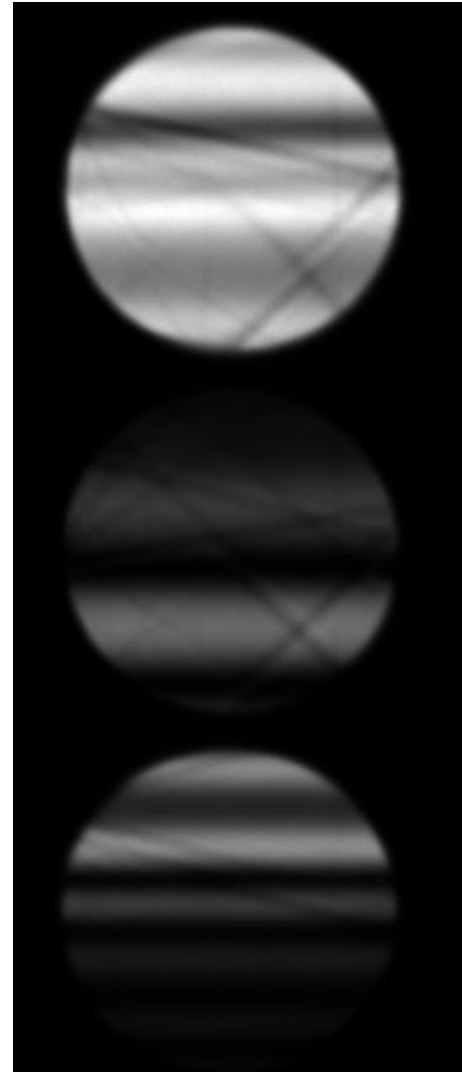
3000 Å

Outline

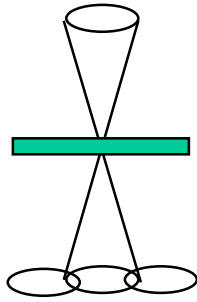
- **Introduction to electron diffraction**
 - Basics in diffraction
 - Electron versus X-ray diffraction
 - SAED → CBED; geometry of CBED
- **Kinematic & dynamic (many beam) simulations**
 - Kinematic diffraction
 - Precession method: Pseudo-kinematic diffraction
 - Dynamical theory; two beam case
- **Experimental considerations**
 - Inelastic scattering, energy filtering
- **Refinement from CBED intensities**
 - Structure factors U_g and their relation to charge density
 - Refining low order U_g using dynamic diffraction intensities
- **Solving structures?**
- **'New' trends**
 - SPED, Scanning CBED, Coherent diffraction - Ptychography

Experimental factors influencing diffraction (CBED) patterns

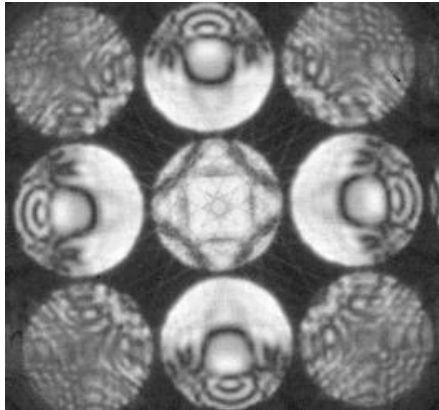
- Microscope alignment
- Orientation of sample
- Convergence angle
- Probe size
- Diffraction focus and stigmatism
- Camera length
- Sample thickness
- Accelerating voltage
- Sample temperature
- Energy filtering
- Recording media
- ...



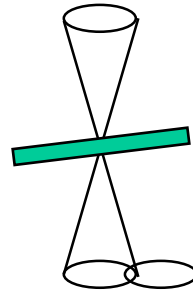
Beam orientations



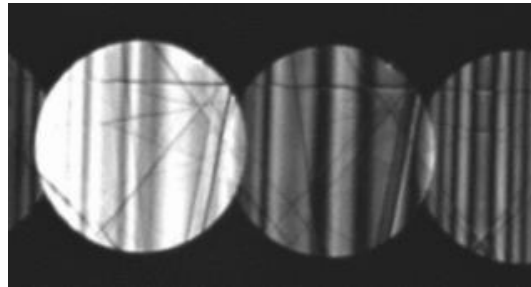
Zone axis



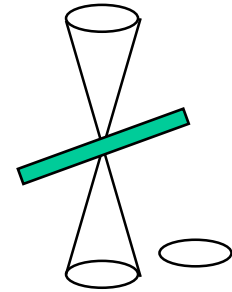
- low order structure factors
- easy to index
- more computation



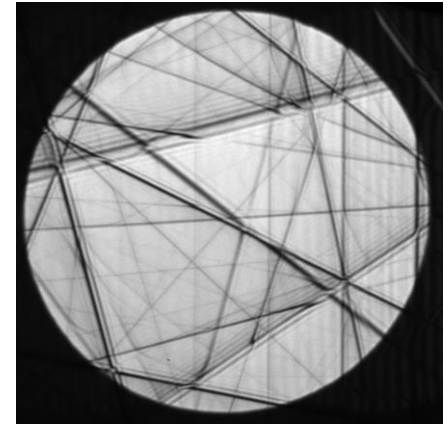
Systematic
low order



- low order structure factors
- difficult to index
- less computation



High angle



- high order structure factors
- atomic positions
- lattice parameters
- Debye-Waller factors

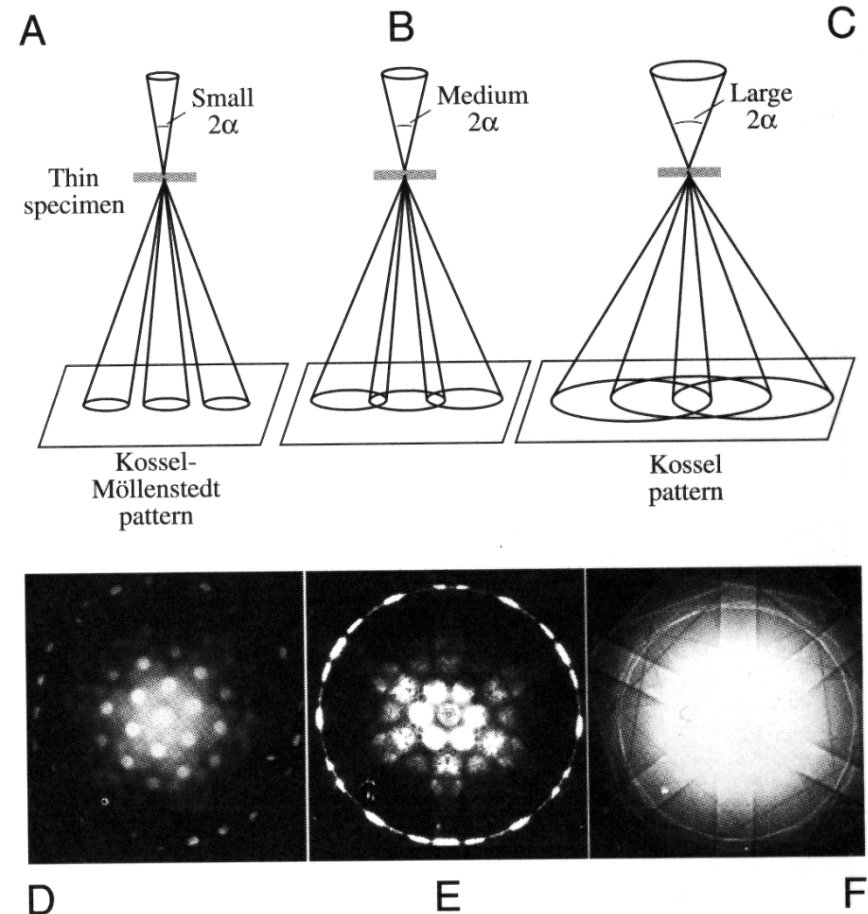
Convergence angle

- Convergence angle $\alpha \Rightarrow$ disc size
 - Condenser aperture size
- \Rightarrow large change of α
- α -selecting lens for smaller changes (on some microscopes)

Resolution:

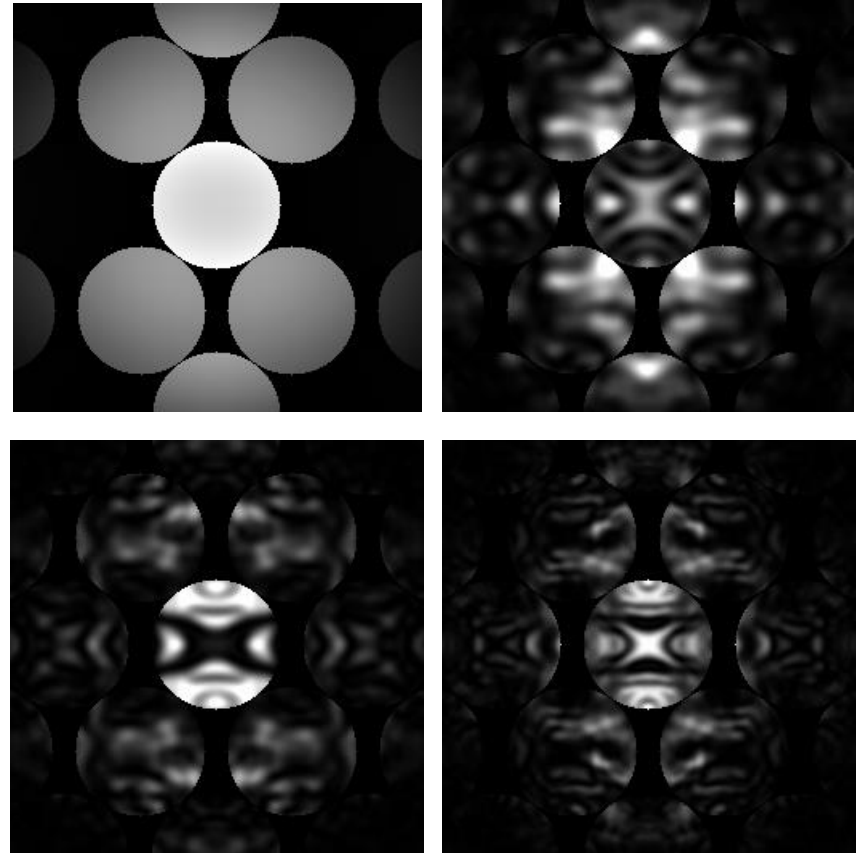
Real Space: Probe size
Probe propagation

Reciprocal Space: Beam divergence



Sample thickness

- Thicker samples create more scattering
- Thicker \Rightarrow more detail inside discs
- Thicker \Rightarrow more inelastic scattering \Rightarrow large background



Accelerating voltage

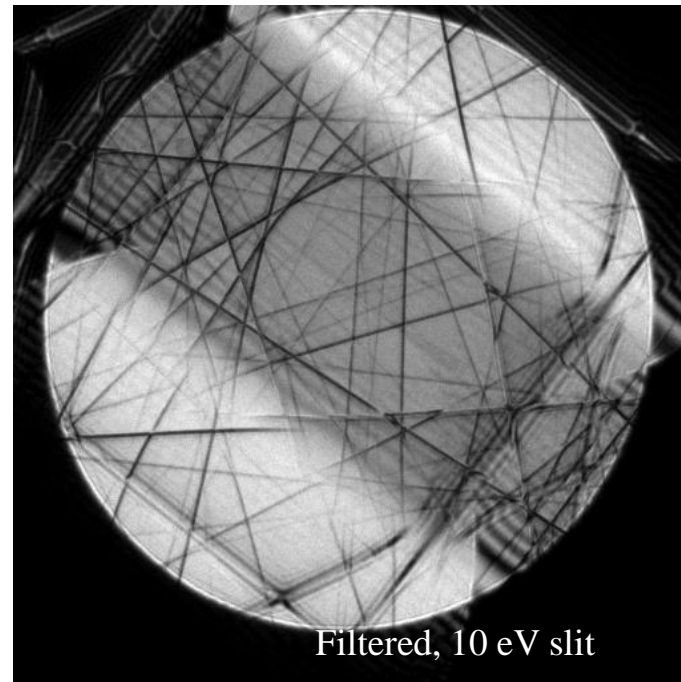
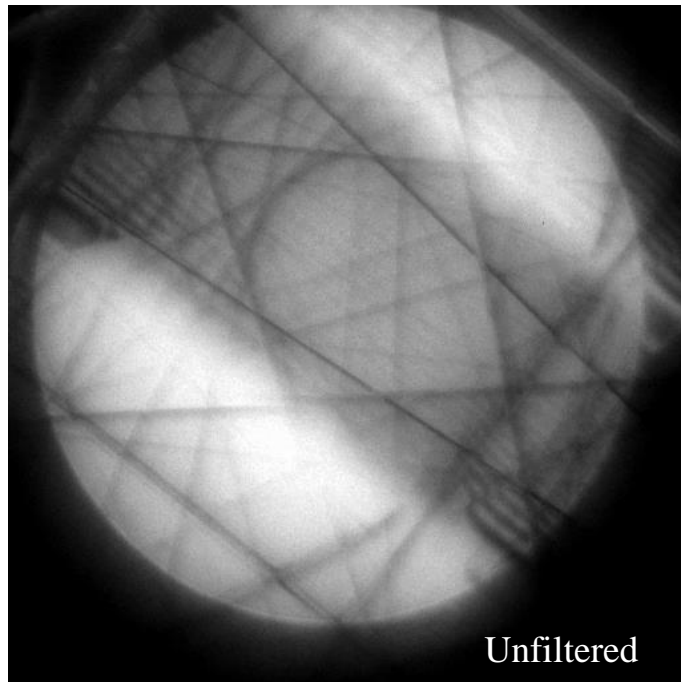
- Higher voltage \Rightarrow less scattering
- Increasing voltage \Rightarrow similar to making sample thinner

Energy filtering - Inelastic scattering

Simulations only include elastic scattering

⇒ Quantitative work must use energy-filtered data!

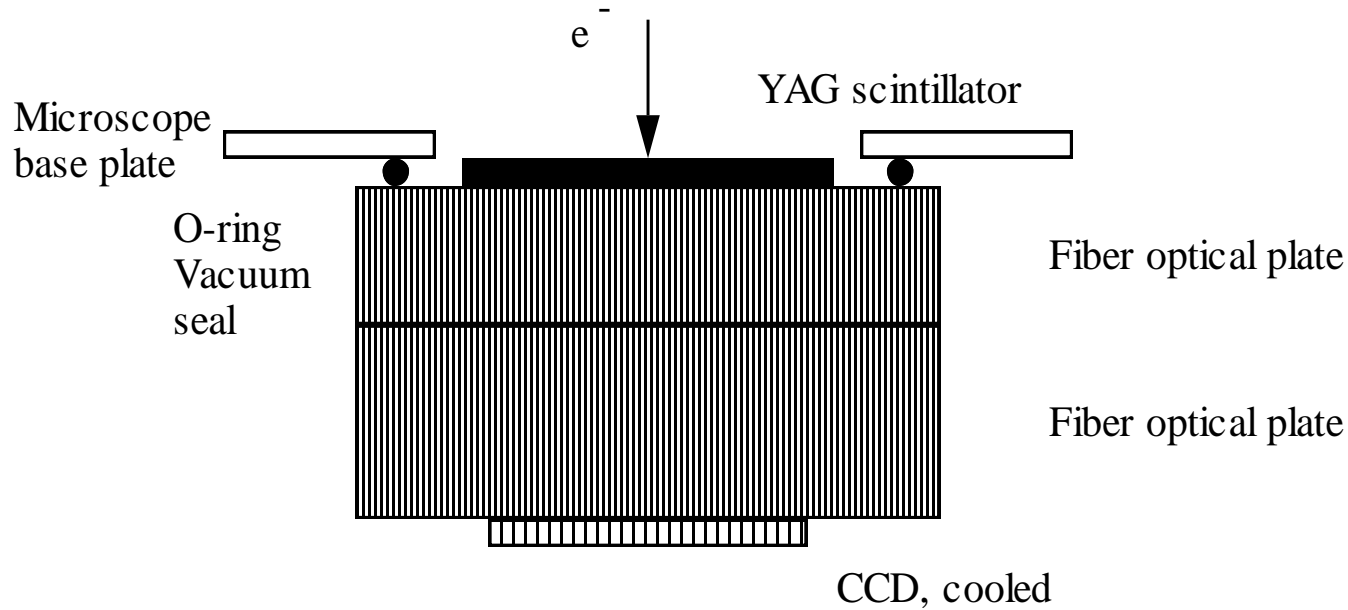
Use in column (Leo, Jeol) or post-column (GIF) filter



Plasmons have the largest contribution to inelastic scattering

Phonons (TDS) cannot be removed, but can be reduced by cooling the sample

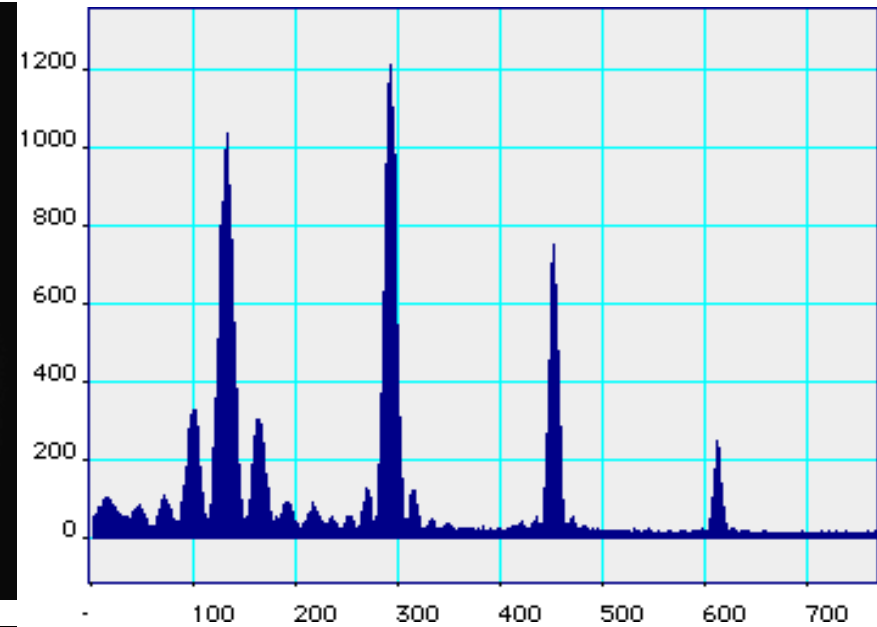
The Effects Introduced by CCD Camera



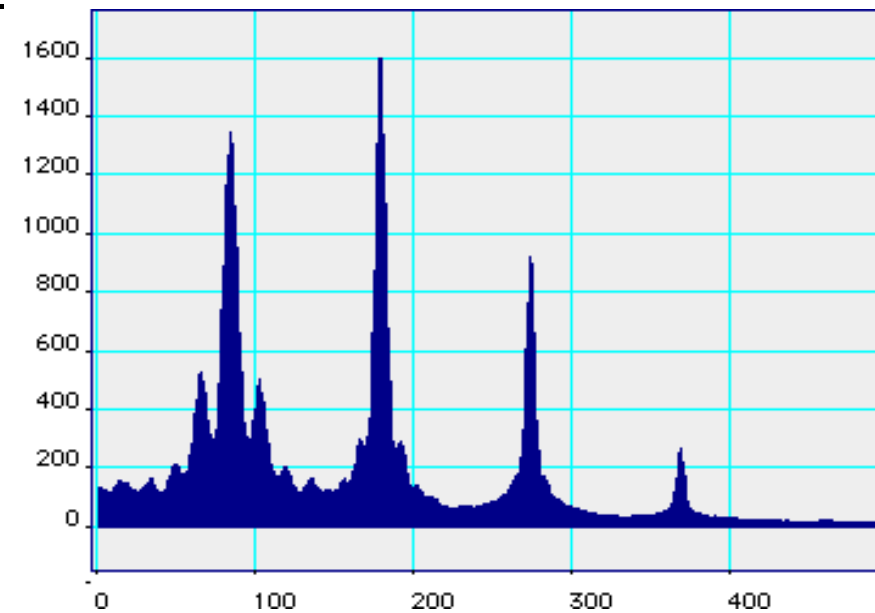
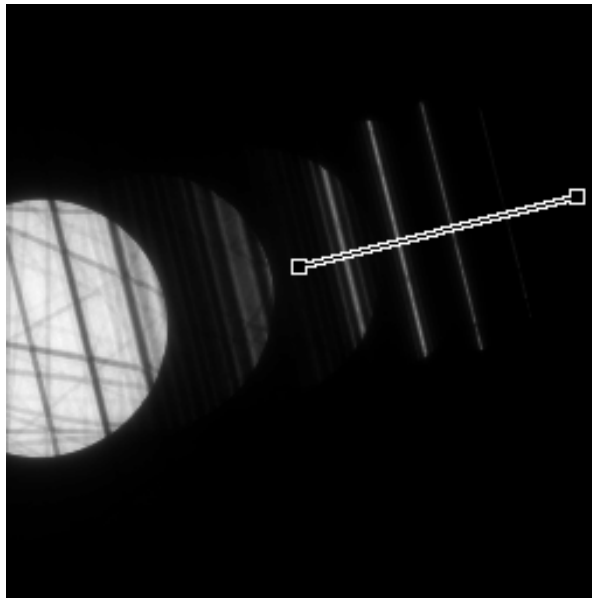
- Gain variation and background intensity -> gain normalization
- Blurring caused by electron and photon scattering -> measurement of MTF
- Noise -> Characterization of detector DQE

As-recorded CBED patterns by the SSC and IP. The large background in the CCD is due the long tail in the point spread function (PSF).

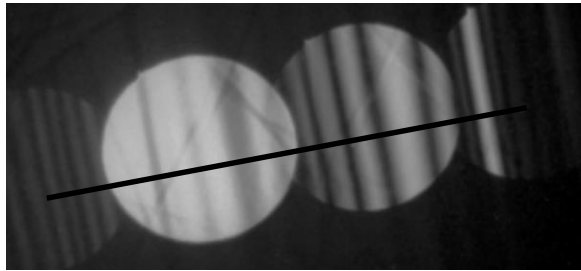
IP
(2048x
2048)



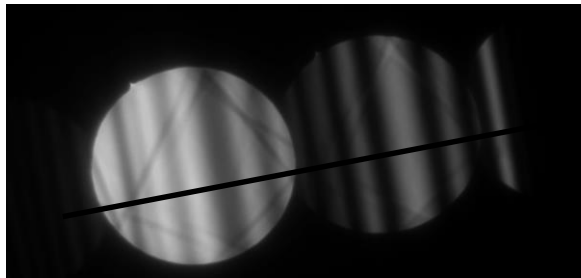
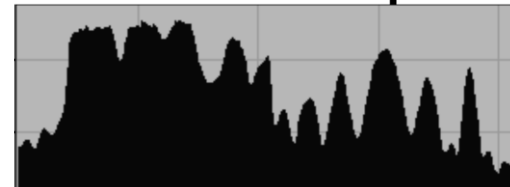
CCD
(1024x
1024)



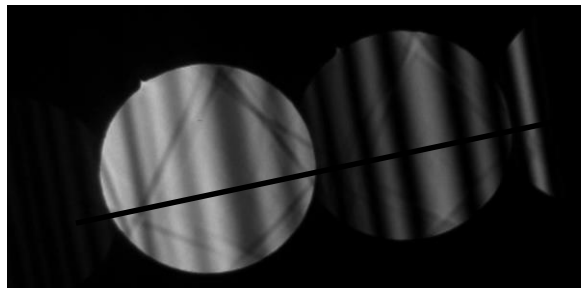
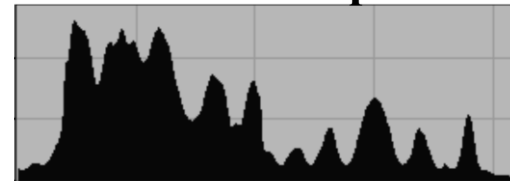
Magnitude of effects



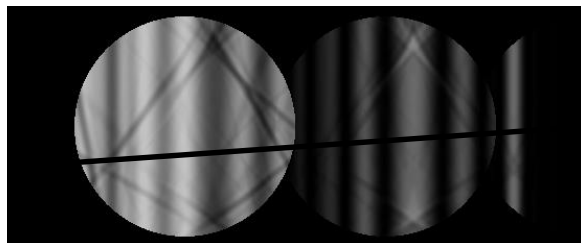
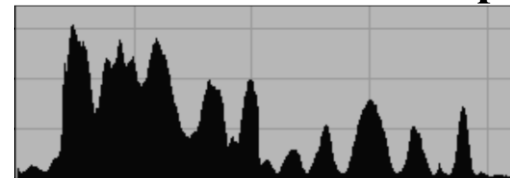
Unfiltered exp.



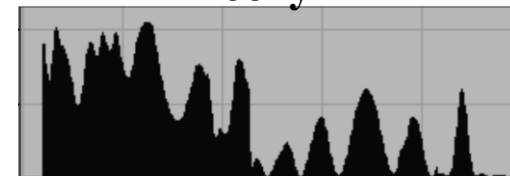
Filtered exp.



Filtered and deconv. exp.



Theory



Outline

- **Introduction to electron diffraction**
 - Basics in diffraction
 - Electron versus X-ray diffraction
 - SAED → CBED; geometry of CBED
- **Kinematic & dynamic (many beam) simulations**
 - Kinematic diffraction
 - Precession method: Pseudo-kinematic diffraction
 - Dynamical theory; two beam case
- **Experimental considerations**
 - Inelastic scattering, energy filtering
- **Refinement from CBED intensities**
 - Structure factors U_g and their relation to charge density
 - Refining low order U_g using dynamic diffraction intensities
- **Solving structures?**
- **'New' trends**
 - SPED, Scanning CBED, Coherent diffraction - Ptychography

Refinements from CBED intensities

Minimise χ^2 :

$$\chi^2 = \frac{1}{n-m} \sum_{i=1}^n \frac{1}{\sigma_i^2} \left[I_i^{\text{experiment}} - I_i^{\text{theory}}(p_1, \dots, p_m) \right]^2$$

i = sampled points inside CBED disks

Parameters p :

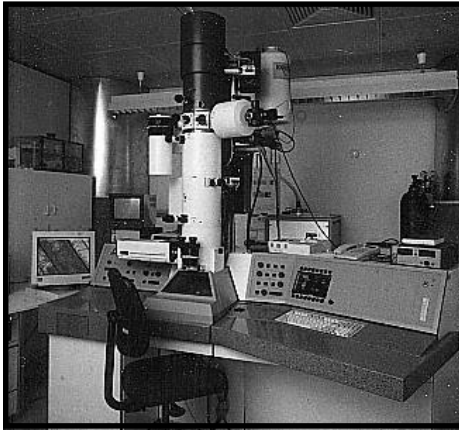
Structure :

- Structure factors; amplitude and phase
- Absorption
- Debye-Waller factors
- Atomic positions / lattice parameters

Geometry:

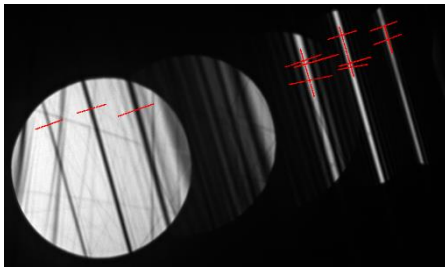
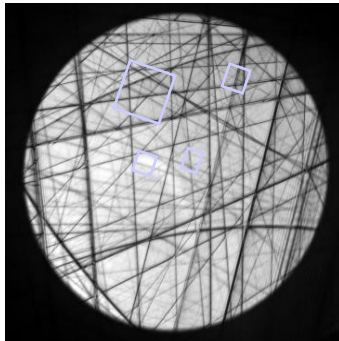
- Beam direction
- Scaling and orientation

Experiment



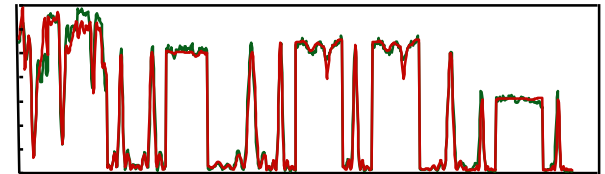
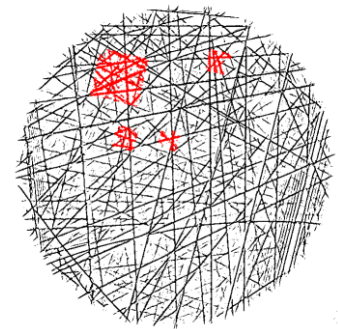
- Cold stage & double tilt specimen holder
- Energy filtering
- Digital recording

Deconvolution
(removal of PSF)



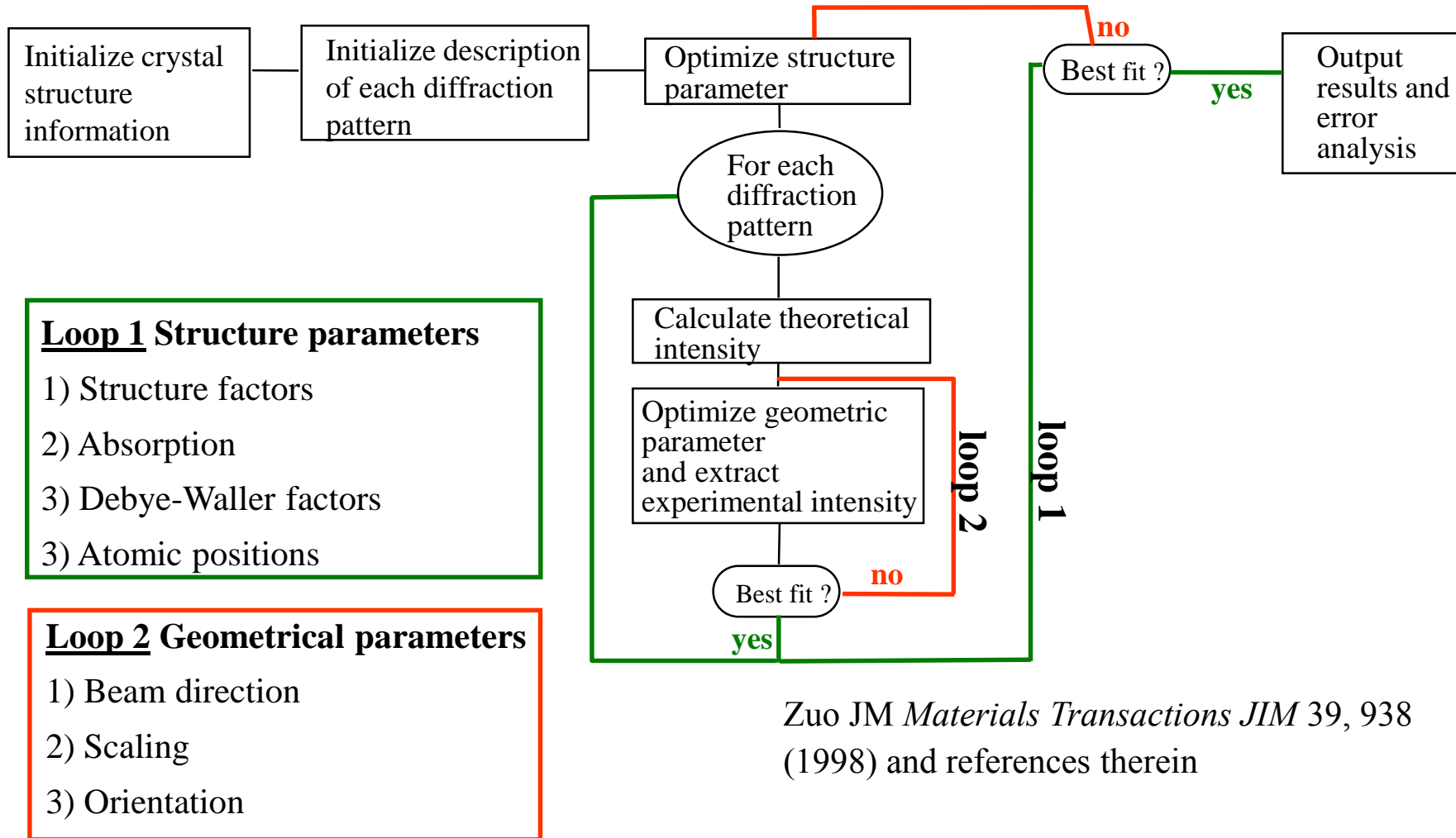
Refinement

s



Analysis and interpretation

Refinement algorithm (JM Zuo)



Zuo JM *Materials Transactions JIM* 39, 938 (1998) and references therein

How to quantify a CBED pattern? (JM Zuo)

1) Determine the crystal orientation

- a) crystal initial orientation and x/y tilts, or
- b) zone axis coordinate

2) Simulate diffraction pattern geometry

- a) Crystal unit cell parameters
- b) Atomic coordinates (not required, but it helps)
- c) Specify the crystal orientation

3) Simulate diffraction intensity

- a) Crystal unit cell parameters
- b) Atomic coordinates (must, if not known, use approximation)
- c) Specify the crystal orientation - the zone axis coordinate
- d) Take account of multiple scattering effects – use dynamic theory (**Bloch wave method** or multislice method)

4) Good diffraction patterns is essential!

- a) crystals, avoid defects, contamination, excessive surface damage layers from ion milling and use small probes for uniform thickness;
- b) choose the right orientation!
- c) reduce detector artifacts.

5) Matching experiment with theory with help of software

Structure factors U_g and their relation to charge density

Electron charge density calculated from

$$\rho_e(\vec{r}) = \frac{1}{\Omega} \sum_g F_g^X \exp(2\pi i \vec{g} \cdot \vec{r})$$

where F_g^X are the X-ray structure factors, in general complex.

Using the Poisson equation, we can from the Mott-Bethe formula find the relationship between the X-ray and the electron structure factors

$$F_g^X = \sum_i Z_i \exp(-2\pi i \vec{g} \cdot \vec{r}_i) - \left(\frac{8\pi^2 \varepsilon_0 \hbar^2 \Omega s^2}{m e^2} \right) U_g$$

(Temperature factor skipped!)

Detailed studies of electron charge distribution and the nature of bonding

Bonding charge density = electron deformation density = difference between electronic distribution in the crystal and that obtained from superposition of spherically symmetric ground state charge densities (procrystal)

$$\Delta\rho(\vec{r}) = \rho_{\text{real crystal}}(\vec{r}) - \rho_{\text{procrystal}}(\vec{r})$$

High order U_g not affected by bonding - Small changes in low order U_g give bonding!
Require very accurate determination of low order structure factors!

Copper

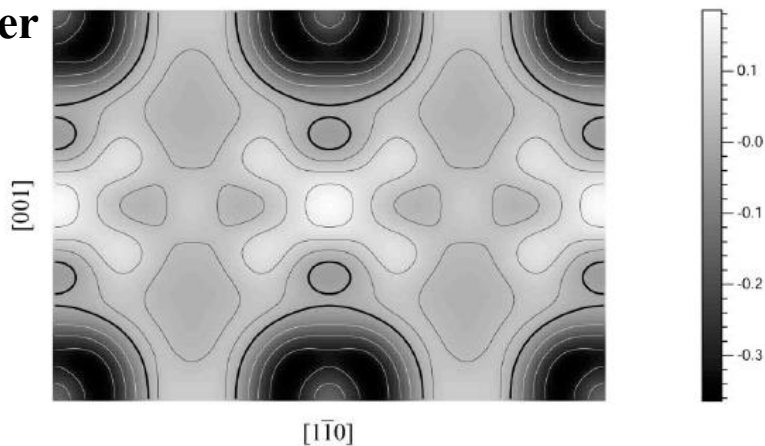


Figure 5

Electron deformation density calculated from the combined data set for $\sin\theta/\lambda < 0.79 \text{ \AA}^{-1}$. Negative contours (white) are at intervals of 0.1 e \AA^{-3} and positive contours (black) are at intervals of 0.05 e \AA^{-3} . The zero contour is shown as a thick line.

- Combine low order structure factors from CBED with medium and high order structure factors from X/ γ -ray!

Friis J, Jiang B, Marthinsen K, Holmestad R
Acta Cryst. A, 61, 223, (2005)

The New York Times

Glue of Molecular Existence Is Finally Unveiled

By MALCOLM W. BROWNE

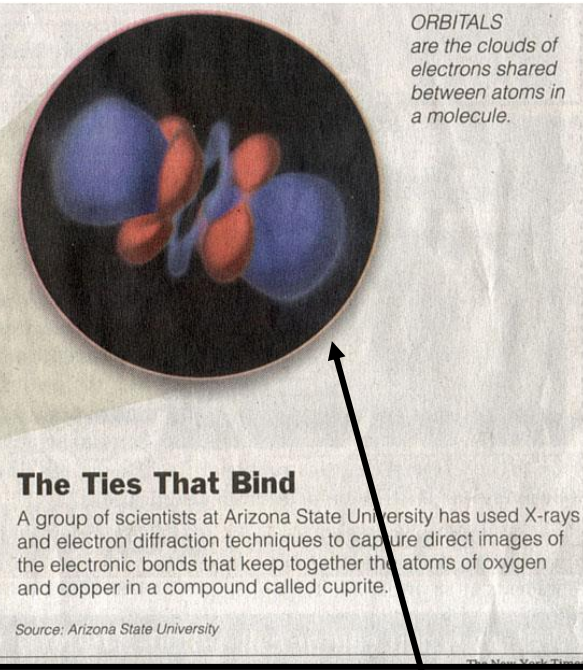
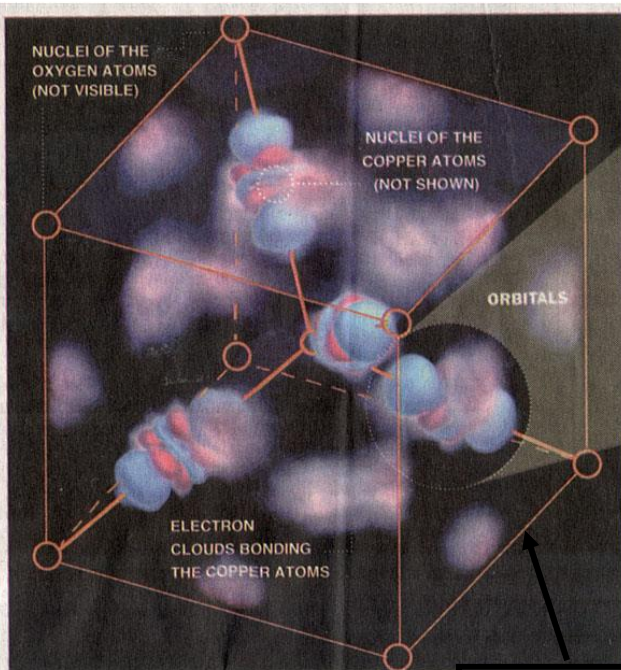
Of the roughly 20 million chemical substances scientists have catalogued, ranging from simple ones like water to gigantic compounds like DNA, nearly all are assemblages of atoms linked together by electronic bonds. The quest to understand these tiny bonds — the very glue of material existence — is the heart of chemical science.

An important step in this quest was reported last week with the publication by the journal *Nature* of the sharpest direct images ever made of electronic bonds (known as orbitals). The shapes revealed by these images — doughnutlike rings, dumbbell-shaped lobes and arrays suggestive of butterfly wings — confirmed theoretical predictions of what these bonds should look like in the molecule under study.

The remarkable pictures also contained fresh evidence bearing on a debate over what kind of bonds may be present in a molecule made of copper and oxygen atoms. Future applications of the new imaging technique, chemists said, may eventually shed light on one of the most intractable mysteries of solid-state physics: why it is that certain compounds of copper and oxygen can conduct electricity without resistance at relatively high temperatures.

Some scientists predict that these "high-temperature superconductors" will underlie much of the technology of the 21st century.

The imaging of bonds was achieved by a team of chemists and physicists at Arizona State University, Tempe, headed by Dr. John C. H. Spence and Dr. Jian-Min Zuo, and



financed by the National Science Foundation. Their technique, using beams of both X-rays and electrons to probe molecules, was the first system capable of imaging both the atoms in a crystal lattice and the electron bonds holding them together.

It was once thought that an atom was like a miniature solar system, with planetary

ele
cle
tur
kno
abo
in s
is m
size

**experimental difference map between
crystal charge density and
superimposed spherical ions,
- blue negative - red positive**

JM Zuo, M Kim, M O'Keeffe and JCH Spence,
Nature 401, 49-52 (1999)

Accurate low order structure factors for Mg

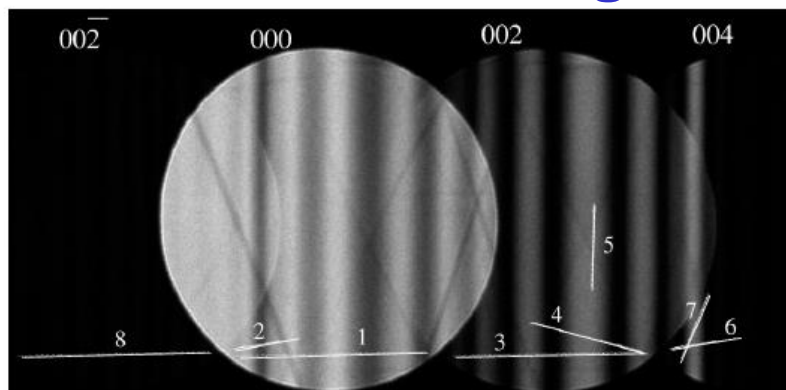


FIG. 2. CBED pattern of the (002) systematic row in magnesium. Eight rocking curves sensitive to the refined parameters are marked on the pattern.

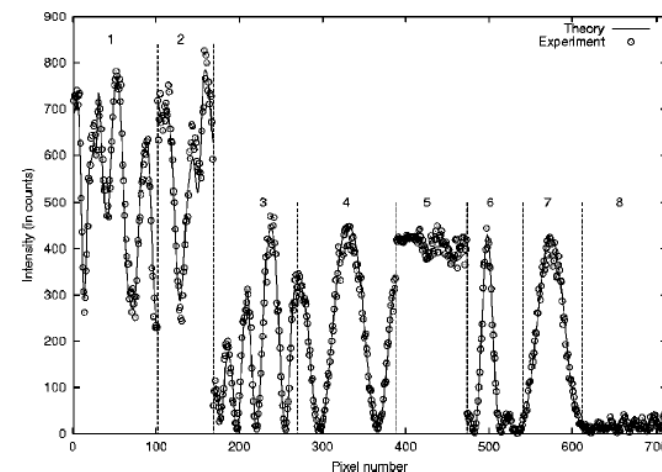


FIG. 3. Best fit between experimental (points) and theoretically calculated (lines) intensities after structure factor refinement of the (002) systematic row CBED pattern shown in Fig. 2. Seven hundred and twelve pixels along the rocking curves drawn on Fig. 2 were included in the refinement. Pixels belonging to different rocking curves are separated by vertical lines. The χ^2 for this particular refinement is 1.47.

TABLE I. Refinement results. The series is continuous up to (210) except for the missing (112) structure factor ($\sin \theta/\lambda = 0.368 \text{ \AA}^{-1}$), for which the CBED patterns suffered from contamination. U are the experimental measured electron structure factors with absorption part U' , while F^0 are the converted static lattice x-ray structure factors. % $\sigma(U)$ and % $\sigma(F^0)$ are the standard deviations (in percentage). Note the reduced standard deviations in the conversion of electron structure factors to x-ray structure factors for the low-order reflections ($\sin \theta/\lambda < 0.35 \text{ \AA}^{-1}$). n is the number of refinements performed for each structure factor. Sample I is the single crystal from the University of Aarhus and II is the Mg ribbon.

h k l	$\sin \theta/\lambda$	U	U'	F^0	% $\sigma(U)$	% $\sigma(F^0)$	n	Sample
1 0 0	0.181	0.018 45(7)	0.000 35	9.01(1)	0.41	0.14	7	II
0 0 2	0.193	0.034 69(4)	0.000 57	17.56(6)	0.12	0.04	6	I
1 0 1	0.205	0.027 96(9)	0.000 23	14.92(2)	0.33	0.13	8	II
1 0 2	0.264	0.011 53(5)	0.000 32	7.90(2)	0.45	0.24	5	I
1 1 0	0.313	0.018 58(2)	0.000 87	14.59(2)	0.16	0.12	5	II
1 0 3	0.341	0.014 38(3)	0.000 44	12.01(2)	0.27	0.20	3	I
2 0 0	0.361	0.007 721(2)	0.000 31	6.68(1)	0.20	0.21	7	II
0 0 4	0.385	0.014 10(3)	0.000 60	12.74(3)	0.25	0.24	6	I
2 1 0	0.478	0.005 242(2)	0.000 23	5.29(2)	0.30	0.49	3	I
2 0 4	0.528	0.004 471(2)	0.000 23	4.74(2)	0.36	0.60	3	I
2 2 0	0.626	0.006 70(5)	0.000 32	7.76(1)	0.80	1.74	2	II

Outline

- **Introduction to electron diffraction**
 - Basics in diffraction
 - Electron versus X-ray diffraction
 - SAED → CBED; geometry of CBED
- **Kinematic & dynamic (many beam) simulations**
 - Kinematic diffraction
 - Precession method: Pseudo-kinematic diffraction
 - Dynamical theory; two beam case
- **Experimental considerations**
 - Inelastic scattering, energy filtering
- **Refinement from CBED intensities**
 - Structure factors U_g and their relation to charge density
 - Refining low order U_g using dynamic diffraction intensities
- **Solving structures?**
- **‘New’ trends**
 - SPED, Scanning CBED, Coherent diffraction - Ptychography

What about solving unknown structures?

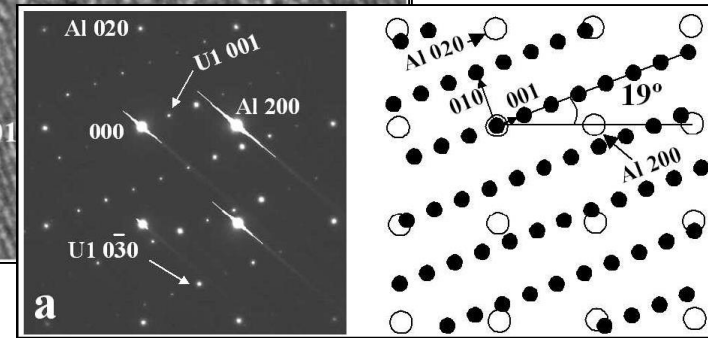
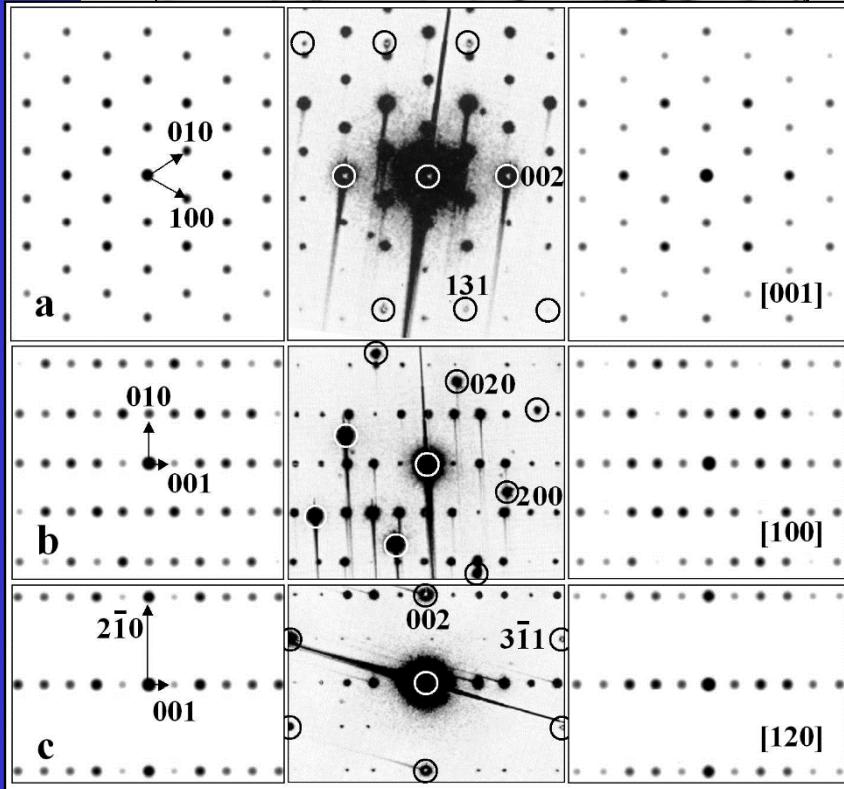
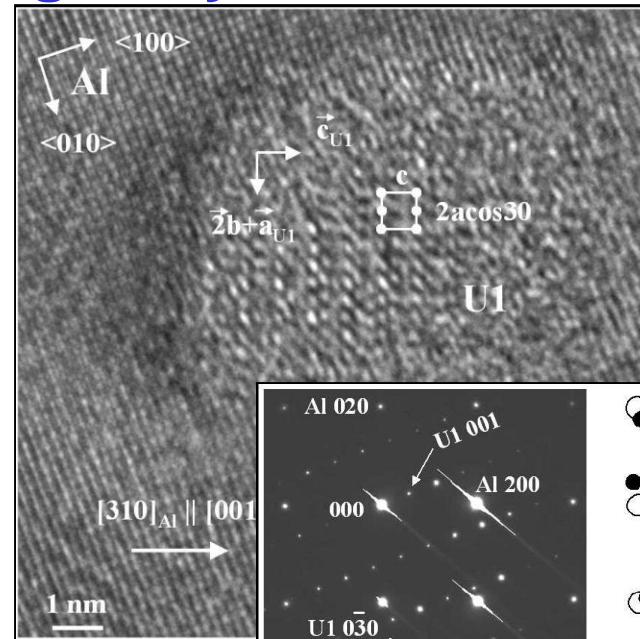
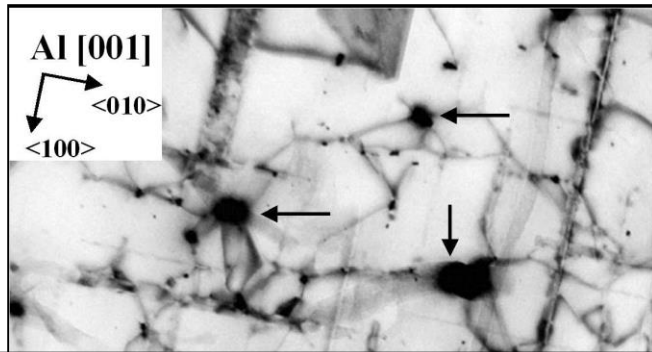
No straight forward method in electron diffraction (yet!!)
often a combination of HREM, STEM, DFT and diffraction.

Often two steps:

- 1) find an approximate **model**. Use EM-images - few reflections, phases.
- 2) **Refine** the model. Use SAED or CBED data - many reflections, only amplitudes.

Marks, Dorset, Gilmore, Saxton, Midgley & Vincent, Hovmøller & Zou, Jansen & Zandbergen.....

Atomic Structure of the trigonal U1-MgAl₂Si₂ Precipitates in the Al-Mg-Si system.



Combination of HREM, EDS, MSLS, DFT ...

MSLS: Jansen, Tang, Zandbergen, Schenk, (1998), *Acta Cryst. A* 54, 91.

WIEN2k: Blaha, Schwarz, Madsen, Kvasnicka, Luitz (2001)

“The challenge of electron crystallography –

In the age of nanoscience, there is an urgent need for a method of rapidly solving new , inorganic nanostructured materials. Many are fine-grained, light element, crystallites which cannot be solved by XRD. The unsolved challenge of 50 years is.....

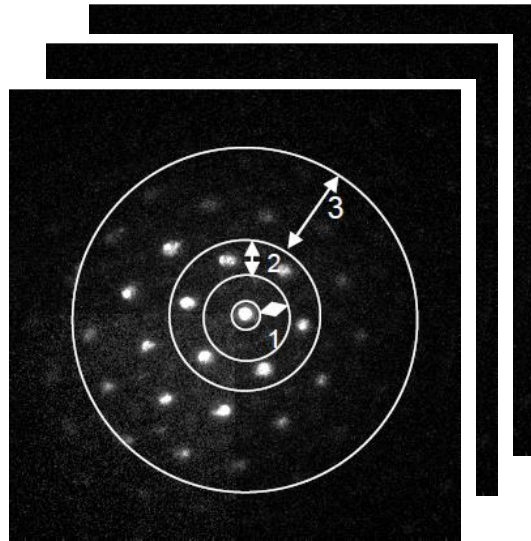
- To collect three-dimensional diffraction data under kinematic conditions
- To solve the same unknown structure first by TED and then by XRD, get same result.”

John Spence, 2004

Outline

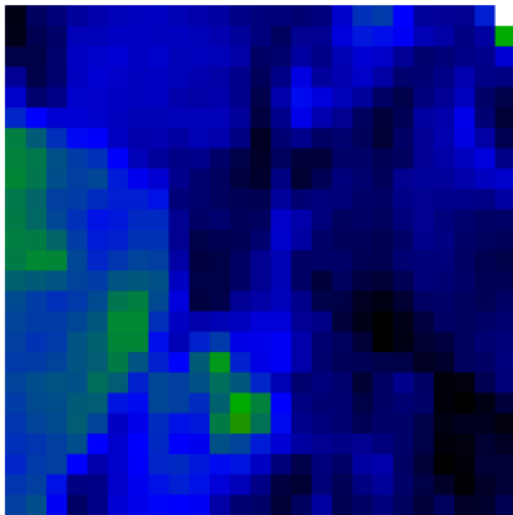
- **Introduction to electron diffraction**
 - Basics in diffraction
 - Electron versus X-ray diffraction
 - SAED → CBED; geometry of CBED
- **Kinematic & dynamic (many beam) simulations**
 - Kinematic diffraction
 - Precession method: Pseudo-kinematic diffraction
 - Dynamical theory; two beam case
- **Experimental considerations**
 - Inelastic scattering, energy filtering
- **Refinement from CBED intensities**
 - Structure factors U_g and their relation to charge density
 - Refining low order U_g using dynamic diffraction intensities
- **Solving structures?**
- **'New' trends**
 - SPED, Scanning CBED, Coherent diffraction - Ptychography

From diffraction patterns to images

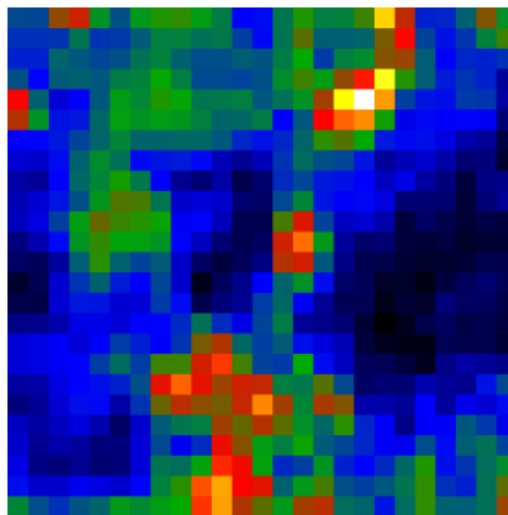


Phase mapping
Symmetry mapping

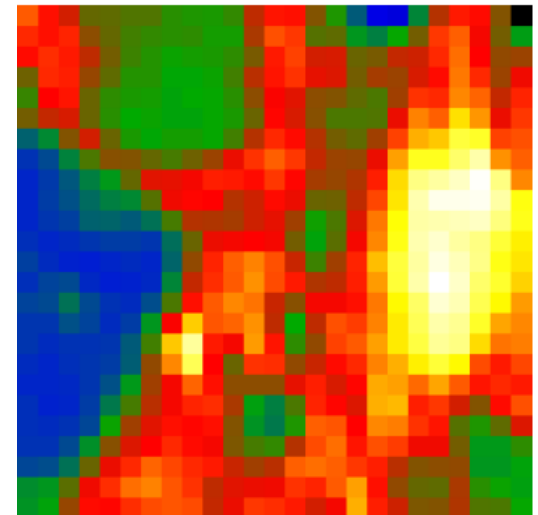
1st



2nd

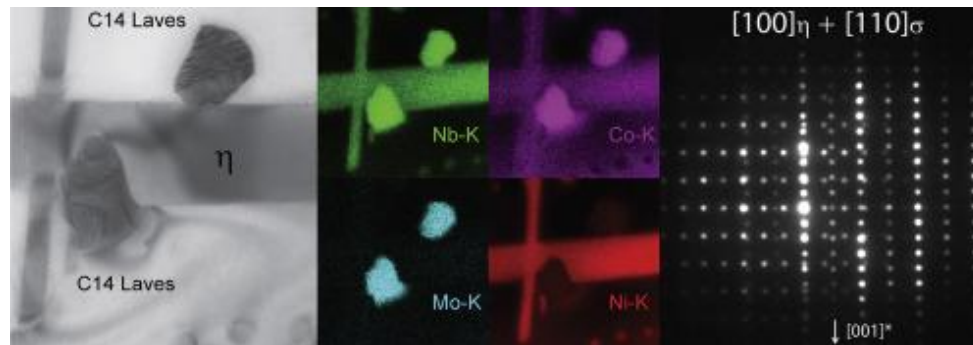
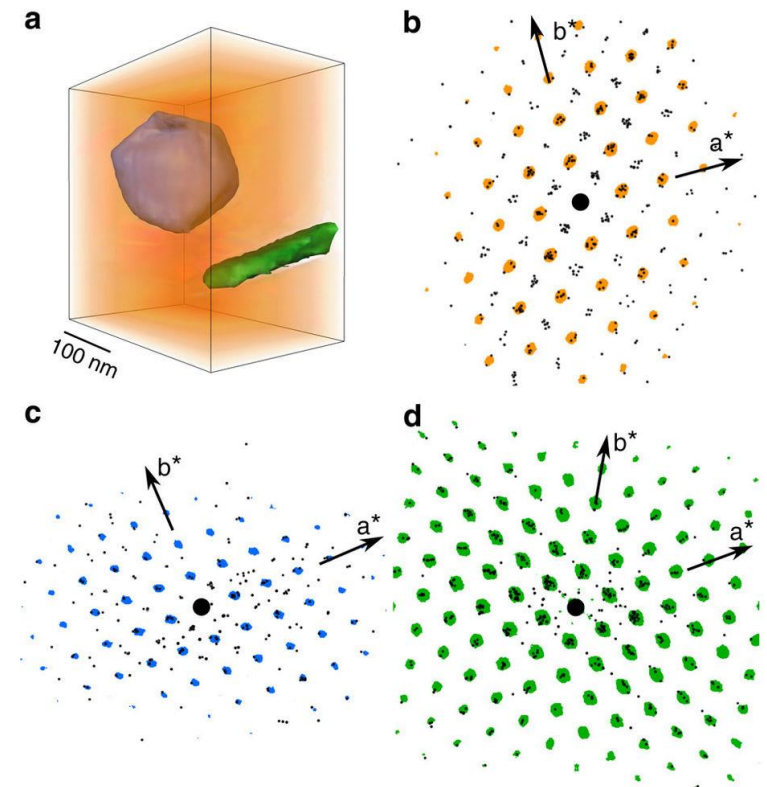


3rd

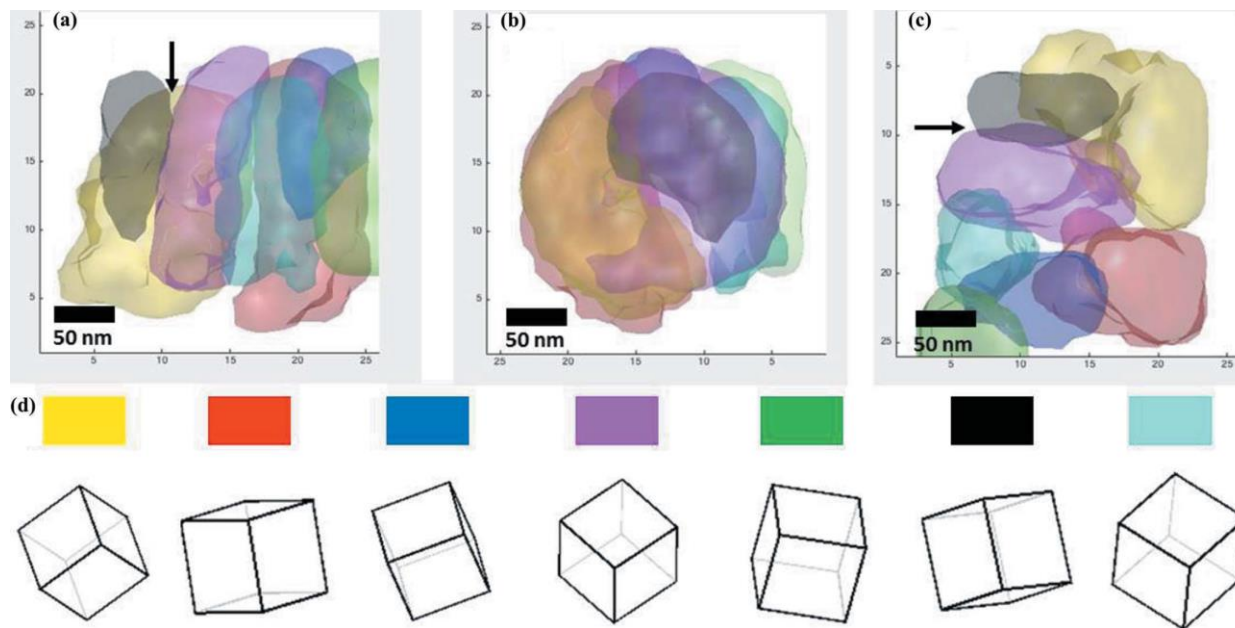


JM Zuo

Scanning precession electron tomography for three-dimensional nanoscale orientation imaging and crystallographic analysis

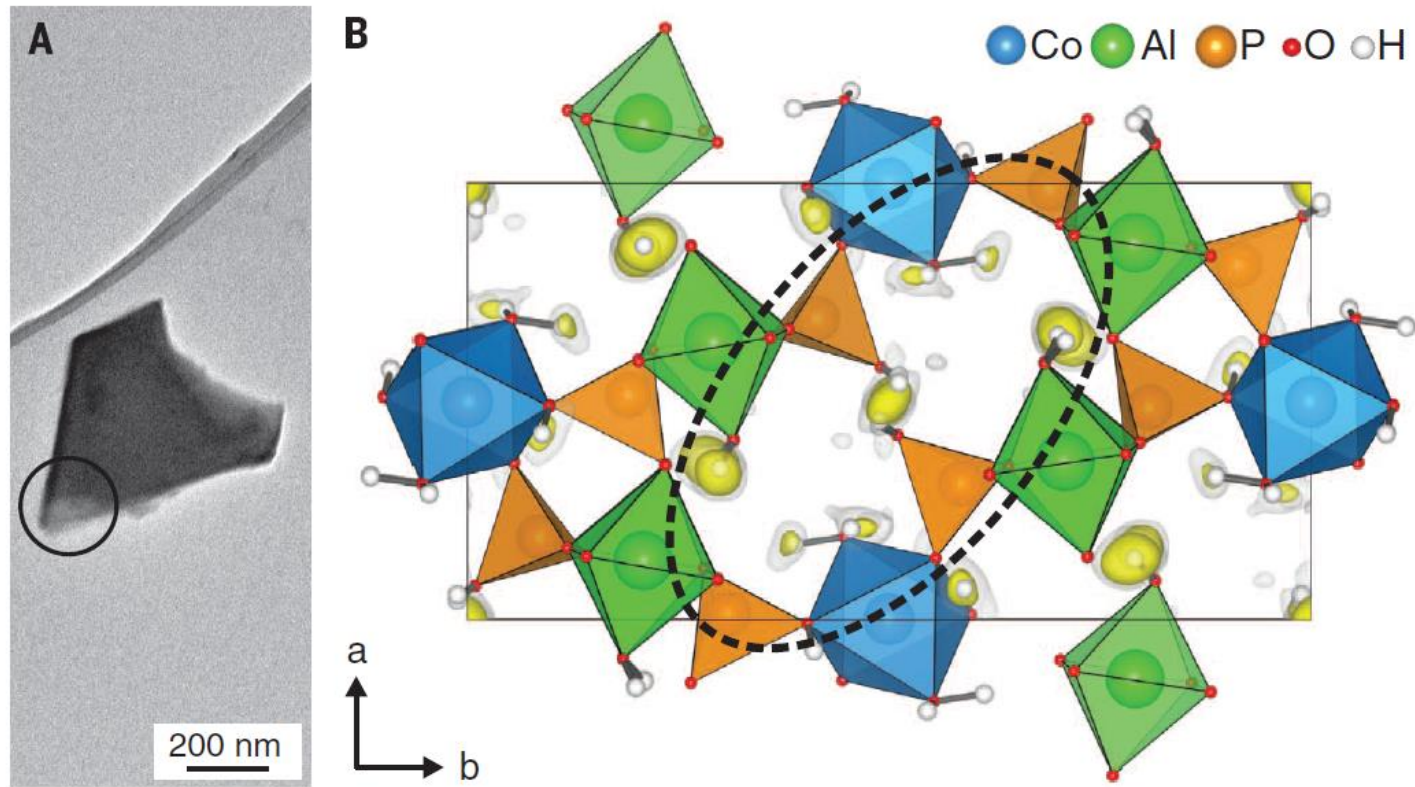


Three-dimensional nanostructure determination from a large diffraction data set recorded using scanning electron nanodiffraction



Meng, Zuo, IUCRJ, 3, 300 (2016)

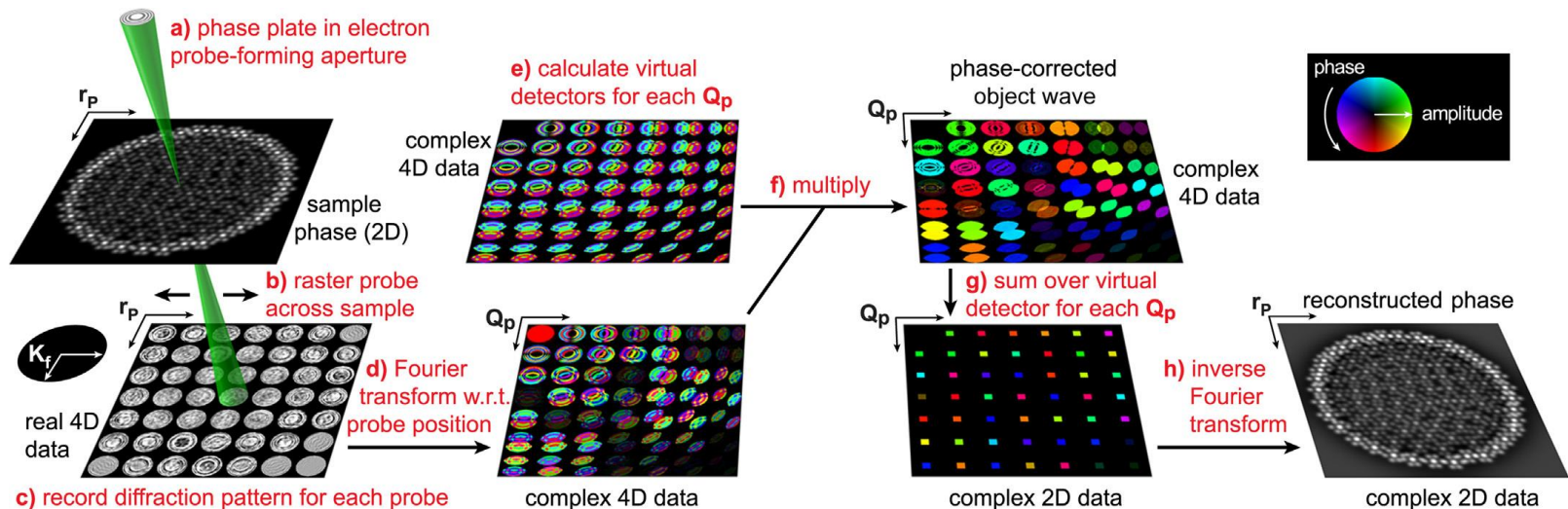
Dynamical refinement of precession electron diffraction tomography data



Palatinus et al., Science 355, 166-169 (2017)

Enhanced phase contrast transfer using ptychography combined with a pre-specimen phase plate in a scanning transmission electron microscope

In this work we introduce a new phase contrast imaging method in a scanning transmission electron microscope (STEM) using a pre-specimen phase plate in the probe forming aperture, combined with a fast pixelated detector to record diffraction patterns at every probe position, and phase reconstruction using ptychography.



Yang, Ercius, Nellist, Ophus, Ultramicroscopy, 171, 117 (2016) .

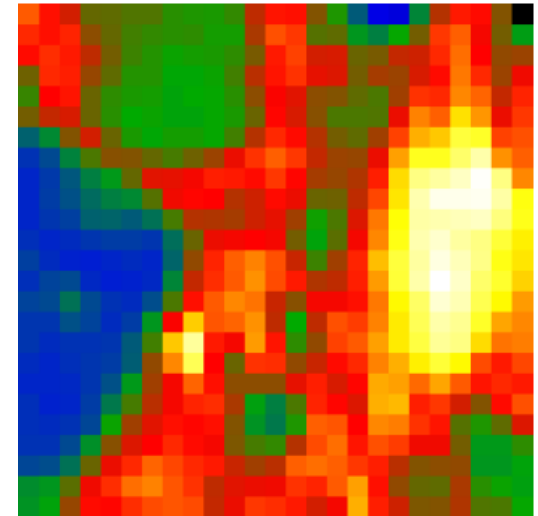
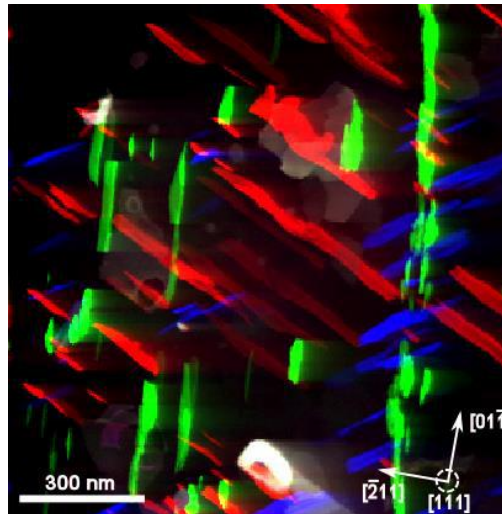
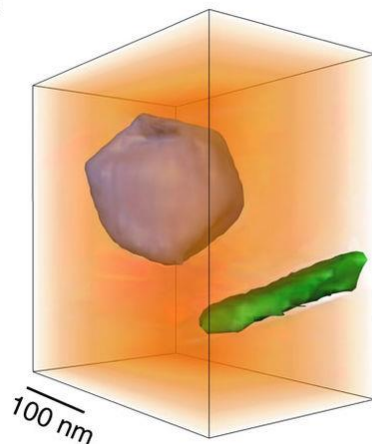
Summary

It is possible to:

- collect high quality electron diffraction intensities from single crystals using CBED.
- simulate them with accuracy down to counting statistics.
- extract quantitative structural information by electron diffraction refinement.

New development in pixelated, fast detectors, possibilities of acquiring multi-dimensional data sets and handling big data has brought /will bring us to a new era in electron diffraction.

a



Many of the images and figures in this presentation are 'stolen' from others –

Thanks to

Jian Min Zuo, University of Illinois at Urbana-Champaign

Martin Saunders, University of Western Australia

John Spence, Arizona State University

Ragnvald Høier NTNU

Knut Marthinsen, NTNU

Jon Gjønnnes, University of Oslo

References –more to read on diffraction and CBED

- Overview: Williams and Carter, *Transmission Electron Microscopy* (1992, Plenum)
- Online: <http://www.matter.org.uk/tem/>
- Complete discussion: Spence and Zuo, *Electron Microdiffraction* (1996, Plenum)
- Lots of examples: Four volumes on CBED by Tanaka (published by JEOL)
- Well written theory: Humphreys, *Rep.Proc.Phys.*, 42, 1825 (1979)
- Useful papers - special issues on electron crystallography:
 - Journal of Electron Microscopy Technique*, Volume 13, Number 1-2 (1989)
 - Microscopy Research and Technique*, Volume 46, Issue 2-3 (1999)
 - Microscopy and Microanalysis*, Volume 9, Issue 5 (2003)